Molecular mobility in amorphous biobased copolyesters obtained with 2,5- and 2,4-furandicarboxylate acid

Aurélie Bourdet, Steven Araujo, Shanmugam Thiyagarajan, Laurent Delbreilh, Antonella Esposito, Eric Dargent

Version of Record: https://www.sciencedirect.com/science/article/pii/S0032386120310508
Manuscript_b5f4b40037c982a4ac67e4b98e8da68b

Molecular mobility in amorphous biobased copolyesters obtained with 2,5- and 2,4-furandicarboxylate acid

Aurélie Bourdet [a], *Steven Araujo*[a], *Shanmugam Thiyagarajan* [b], *Laurent Delbreilh* [a], *Antonella Esposito* [a,*], *Eric Dargent* [a]

[a] Normandie Univ, UNIROUEN Normandie, INSA Rouen, CNRS, Groupe de Physique des Matériaux, 76000 Rouen, France

[b] Wageningen Food & Biobased Research, P.O. Box 17, 6700 AA Wageningen, The Netherlands

* Corresponding author antonella.esposito@univ-rouen.fr

KEYWORDS

Poly(ethylene furandicarboxylate) (PEF); copolymers; position isomerism; Temperature-Modulated Differential Scanning Calorimetry (TM-DSC); Dielectric Relaxation Spectroscopy (DRS); Thermo-Stimulated Depolarization Current (TSDC); fragility; cooperativity; activation energy; relaxation processes

ABSTRACT

Poly(ethylene 2,5-furandicarboxylate) (2,5-PEF) is one of the most credible biobased alternative to poly (ethylene terephthalate) (PET). The Henkel disproportionation reaction that leads to furandicarboxylic acid (FDCA) provides three position isomers: 2,5-FDCA (obtained with the highest yield), 2,4-FDCA (so far considered as a by-product), and 3,4-FDCA (traces). The copolymerization of the two main isomers of FDCA with a diol, e.g. ethylene glycol (EG), is an interesting approach to obtain a family of furan-based biopolymers with adjusted physical properties. This work investigates the molecular mobility of three

copolymers obtained with EG and ratios of 2,5-FDCA and 2,4-FDCA ensuring the complete disruption of crystallization (90:10, 85:15 and 50:50 mol % of 2,5:2,4 FDCA), as compared to the homopolymers 2,5-PEF and 2,4-PEF. The molecular mobility was investigated by cross-comparing the results obtained by Modulated-Temperature Differential Scanning Calorimetry (MT-DSC), Dielectric Relaxation Spectroscopy (DRS) and Thermo-Stimulated Depolarization Currents (TSDC), with the aim of evaluating the local and segmental molecular mobilities, their activation energies, as well as the temperature dependence of the relaxation time and of the cooperatively rearranging regions at the glass transition. The furan ring in 2,5-FDCA (2,5-PEF) has a rotation axis that is less linear compared to the benzene ring in terephthalic acid (PET), with consequences on the ring-flipping mechanisms. 2,5-FDCA and 2,4-FDCA differ by the position of the carbonyl groups on the furan ring, which adds asymmetry to non-linearity. The incorporation of 2,4-FDCA-based units into a polymer backbone mainly constituted of 2,5-FDCA-based repeating units is responsible for longer relaxation times associated with the local β relaxation processes, no striking effects on the kinetic fragility index m, no obvious effects on cooperativity (a slightly increase in the cooperativity length is observed in the liquid state), no effects on the activation energy for the segmental α relaxation in the liquid state, and a decrease in the activation energy in the glassy state.

INTRODUCTION

The awareness about the progressive consumption of fossil resources, along with the concerns about the impact of human activities on the environment, have recently renewed strong interest in the exploration of sustainable resources for energy and materials [1, 2]. Of all the renewable raw materials that can be used to obtain bioplastics, furan-based synthons have attracted considerable attention. The most significant example is 2,5-furandicarboxylic acid

(2,5-FDCA), i.e. the acid used to synthesize poly (ethylene 2,5-furandicarboxylate) (2,5-PEF, most commonly known just as PEF). PEF is currently considered as the most credible biobased alternative to poly (ethylene terephthalate) (PET) [3-8]. Less than ten years ago, Lee et al. [9] developed an advanced gas/vapor permeation system for barrier materials; Burgess et al. have then reported promising results about the transport properties of PEF as compared to PET for different permeants [10-12]. As for the microstructure, both quiescent and strain-induced crystallization of 2,5-PEF have been studied [13-18]. Stoclet et al. [13] evaluated the influence of the crystallization temperature (T_c) on the degree of perfection of the crystalline phase, and found that a disordered α' crystalline phase is formed at low temperature (T_c < 170 °C) whereas the ordered α crystalline phase is formed at higher temperature (T_c > 170 °C). They also found that the crystalline structure induced upon stretching differs from the one observed after crystallization under quiescent conditions, for stretched 2,5-PEF macromolecules crystallize while being in their extended state [17]. Burgess et al. [19] had previously evidenced that the furan ring-flipping mechanism in PEF is greatly suppressed with respect to the active phenyl ring-flipping mechanism in PET, thereby reducing β relaxation motions and diffusion due to the energy penalty associated with the non-linear axis of ring rotation and ring polarity. Recently, Araujo et al. [20] provided an explanation to the improved barrier properties of 2,5-PEF compared to PET based on the vibrational modes involving the furanic ring, which also increases the stiffness of the polymer backbone. They showed that 2,5-PEF macromolecules are most likely found in a helical conformation in the amorphous domains, whereas in the crystalline domains they arrange in a zig zag conformation; the energy difference between the conformations of 2,5-PEF chains in the amorphous and crystalline phases is 3 times higher than for PET chains, which explains the higher crystallization temperature of 2,5-PEF as compared to PET. These results all reinforce the idea that 2,5-PEF is a good candidate to replace PET for packaging.

The association of different repeating units is a strategy commonly used to adjust the properties of polyesters through the control of their composition arrangement [21-25]. The possibility of associating the repeating units of PET and 2,5-PEF has already been investigated [6, 21]. This association provides a copolyester (PETF) with lower crystallization rates and increased stiffness as the concentration of ethylene 2,5-furanoate units in the PET backbone increases, following a trend that appears even at small degrees of copolymerization [6, 26]. A review has recently been published by Terzopoulou et al. [27] summarizing the attempts that have been done so far for tuning the properties of furandicarboxylic acid-based polyesters through copolymerization. Thiyagarajan et al. [28, 29] recently reported that the one-pot Henkel-type disproportionation reaction to obtain furandicarboxylic acid actually provides three position isomers of FDCA: 2,5-furandicarboxylic acid (2,5-FDCA), 2,4-furandicarboxylic acid (2,4-FDCA) and 3,4-furandicarboxylic acid (3,4-FDCA). 2,5-FDCA is the isomer produced with the highest yield (70%), but the yield observed for 2,4-FDCA is also interesting (30%), whereas 3,4-FDCA is only obtained in the form of traces (< 5%). Interestingly, the position of the carbonylic group on the furan ring has no influence on the reactivity of these isomers, as proved by the fact that all of them could equally lead to high molecular weight homopolyesters [28-30]. A preliminary comparison of the two homopolymers based on 2,5- and 2,4-FDCA (2,5-PEF and 2,4-PEF respectively) showed that 2,4-PEF has a lower glass transition temperature and a negligible crystallization rate with respect to 2,5-PEF, enough for being classified among amorphous polyesters [29]. A more recent work about these two homopolymers [31] showed that the properties of furan-based polyesters are significantly affected by the position of the carbonyl groups on the furan ring. In particular, the local β relaxations are quite different in 2,4-PEF and 2,5-PEF; the FDCA-based repeating units with an asymmetrical position of the carbonyl

groups on the furan ring require longer times to relax as compared to their symmetrical counterparts. This result goes well with the observations made by Burgess et al. [19] about the furan and phenyl ring-flipping mechanisms in 2,5-PEF and PET, and the influence of the ring rotation axis linearity on the β relaxation motions. Besides the local β relaxations, Bourdet et al. [31] also investigated the structural α relaxation, revealing that 2,5-PEF and 2,4-PEF both behave as fragile glass-forming systems, with m values (116 for 2,5-PEF and 120 for 2,4-PEF) significantly lower compared to other polyesters (142 for PET). Kunal et al. [32] had previously compared the glass-forming behavior of various polymers with different side groups and backbone structures, and found that fragility is mostly influenced by the flexibility of the side groups relative to the flexibility of the backbone. If two polymers are compared having the same side groups but different arrangements in the backbone with possible consequences on flexibility, an increase in the backbone stiffness should produce an increase in the glass transition temperature as well as in the fragility index. However, the glass transition temperature of a polymer is not only related to segmental mobility, but also to specific interactions that can be established between the chains, in particular dipole-driven interactions. Interestingly, Bourdet et al. [31] reported a significant difference in the dielectric strength of 2,5-PEF and 2,4-PEF, at first measured by dielectric relaxation spectroscopy and subsequently confirmed by molecular dynamics simulations (the average dipole moment is 8.2 D for 2,5-PEF vs. 6.2 D for 2,4-PEF). Thiyagarajan et al. [30] recently reported that a family of copolyesters can be obtained by using mixtures of the two main FDCA isomers. Preliminary results showed that the presence of 2,4-FDCA-based repeating units among the 2,5-FDCA-based repeating units results in a decrease of the glass transition temperature T_g and a crystallinity disruption as compared to 2,5-PEF. Due to the complex dependence of the glass transition temperature on the chemical composition and arrangement of the subunits in furan-based copolyesters, the authors used different mixing laws to fit the values of T_g plotted

against the content of 2,5-FDCA-based repeating units; the best results were obtained with Gordon-Taylor's and Kwei's equations, which are models taking into account the eventual unequal contributions of each isomer to the value of T_g and the presence of specific dipole-driven interactions, respectively.

This work aims at further investigating the influence of the position isomerism of FDCA (that is to say, the influence of symmetry and non-linearity of the ring rotation axis, as determined by the position of the carbonyl groups on each side of the furan ring) on the properties of amorphous furan-based copolyesters. To this purpose, different mixtures of 2,5- and 2,4-FDCA (90:10, 85:15 and 50:50 mol %) were used in combination with ethylene glycol (EG) to obtain three copolyesters, that were then compared with the two homopolymers (2,5-PEF and 2,4-PEF).

Most properties of amorphous polymers are related to the nature of the molecular movements, both in the glassy and the liquid states. Molecular mobility depends on temperature; it decreases as temperature decreases, and eventually becomes cooperative as a consequence of the viscous slowing down observed in supercooled liquids. Cooperativity was first introduced by Adam and Gibbs [33], who defined a Cooperative Rearranging Region (CRR) as the smallest subsystem that, provided a sufficient thermal fluctuation, is able to undergo conformational rearrangements independently of its environment. The CRR concept has recently been used to describe the molecular dynamics at the glass transition of a wide range of more or less complex polymer systems [34-38] according to Donth's experimental approach [39], which is only based on calorimetric measurements, and has been successfully extended to temperatures above T_g with the contribution of relaxation dielectric spectroscopy [40]. Codou et al. [41] investigated the glass transition dynamics and cooperativity length of 2,5-PEF compared to PET at different crystallinities by stochastically modulated differential

scanning calorimetry and dynamic mechanical analysis. For amorphous 2,5-PEF, they reported a higher value of the heat capacity step at the glass transition, a broader relaxation spectrum attributed to a higher free volume, and similar lengths of the cooperative rearranging regions. They also evaluated the variations of the effective activation energy at the glass transition by isoconversional kinetic analysis, and found that the rate of decrease was similar for both the amorphous polyesters. Ginzburg [42] has just published a paper proposing a new phenomenological model describing the equilibrium glassy dynamics of amorphous materials with two fundamental assumptions, that (1) the CRR can have two possible states ("solid" and "liquid"), and (2) the diffusion/relaxation activation energy of the "solid" state is much larger than the "liquid" state. The glass transition is therefore described as a mean-field continuous transition from a "solid" (high-energy, low-entropy, high-activation energy) to a "liquid" (low-energy, high-entropy, low-activation energy) state, with each CRR going from solid to liquid at a critical temperature defined by thermodynamics. This model has been used to describe the temperature dependence of the relaxation time at high (Arrhenius), intermediate (Williams-Landel-Ferry) and low (low temperature Arrhenius) regimes, and could eventually be used to predict the relaxation dynamics in polymer blends and copolymers.

In this work, the cooperativity associated with the molecular movements responsible for the structural α relaxation was evaluated by Modulated Temperature Differential Scanning Calorimetry (MT-DSC); the relaxation times were measured both below and above the glass transition by Thermally Stimulated Depolarization Current (TSDC) and Dielectric Relaxation Spectroscopy (DRS), respectively; the relaxation dynamics of both the segmental (α) and local (β) relaxation processes were investigated, providing information about the influence of FDCA position isomerism on the fragility index characteristic of the α relaxation and the activation energies of both the α and β relaxation processes.

EXPERIMENTAL SECTION

Materials and methods

The synthesis of poly (ethylene 2,5-furandicarboxylate) (2,5-PEF), poly (ethylene 2,4-furandicarboxylate) (2,4-PEF) and random poly(ethylene 2,5-*co*-2,4-furandicarboxylate) (2,5/2,4-PEF) copolymers with different ratios of 2,5-FDCA (90, 85 and 50 mol %) has already been described in previous works [28, 30]. The chemical structures, the weight-average molecular weights ($\overline{M_w}$) and the number-average molecular weights ($\overline{M_n}$) determined by gel permeation chromatography are reported in Table 1. All the polyesters investigated in this work have reasonably high molecular weights even without solid-state post-condensation reaction (similar values of the glass transition temperature were previously reported for different batches of 2,5-PEF and 2,4-PEF with much higher molecular weights, suggesting that the threshold of the critical molecular weight is passed in this work too [29]), with values of dispersity ranging between 1.7 and 2.5.

Table 1. Ratios of 2,5-FDCA DME measured by Nuclear Magnetic Resonance (NMR), along with the values of weight-average molecular weight ($\overline{M_w}$) and number-average molecular weight ($\overline{M_n}$) measured by gel permeation chromatography (GPC), for the homopolymers 2,5-PEF and 2,4-PEF, as well as the three random copolyesters obtained with both 2,5- and 2,4-FDCA.

Sample	Repeating unit	2,5-FDCA DME ratio (%)	$\overline{M_w}$ (kg/mol)	$\overline{M_n}$ (kg/mol)
2,5-PEF	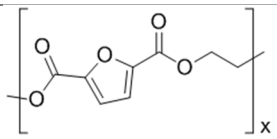	100	18.2	15.3
PE-2,5[90]-2,4[10]F	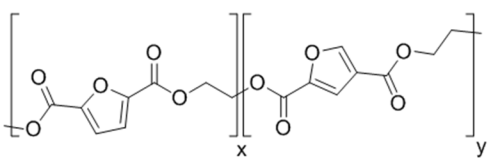	90	14.7	9.1
PE-2,5[85]-2,4[15]F		85	15.2	9.2

PE-2,5[50]-2,4[50]F		50	23.3	13.2
2,4-PEF	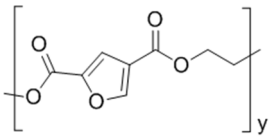	0	11.4	8.5

All the measurements were performed on freshly prepared samples. Prior to characterization, all the samples were dried for 3 days at 95 °C (about $T_g + 15$ °C) to remove any residual solvents used during the synthesis, stored in a desiccator over P_2O_5 until measurement, and quenched to the fully amorphous state. The following quenching protocol was applied to all the samples: (1) a hot plate was stabilized at 215°C (i.e. above the melting temperature), (2) the polymer (powder) was placed in an aluminum pan (for MT-DSC measurements) or distributed all over the golden surface of the electrode until covering the interdigitated comb fingers (for DRS and TSDC measurements), (3) the aluminum pan (or the electrode) was kept at the selected temperature during 2 minutes to remove any possible crystals, and (4) the sample was quenched by transferring the aluminum pan (or the electrode) on a cold metal plate.

Modulated Temperature Differential Scanning Calorimetry (MT-DSC). The calorimeter (Q2000, TA Instruments) was calibrated for temperature and energy using standard indium ($T_m = 156.6$ °C, $\Delta H_m = 28.66$ J/g) and benzophenone ($T_m = 48.0$ °C). The calibration for specific heat capacity was carried out using standard sapphire. MT-DSC experiments were performed with "Heat-Cool" modulation parameters (oscillation amplitude ± 3 K, oscillation period 120 s, and heating rate 1 K/min); these parameters optimize the investigation of the glass transition and the corresponding relaxation phenomena in amorphous polymers [39, 43]. MT-DSC measurements provided the apparent complex heat capacity C^*, successively used to extract the real (in-phase) component of the heat capacity, noted *C'*.

Dielectric Relaxation Spectroscopy (DRS). DRS experiments were performed using interdigitated electrodes (IEs) (DRS1410-20-150, Novocontrol Technologies, with a sensor diameter of 20 mm, gold-plated copper combs, spacing between the comb fingers 150 µm, thickness of the comb fingers 35 µm, and an accuracy in loss factor $\tan\delta = 0.001$). Prior to sample deposition, each electrode was calibrated by measuring its respective geometric (i.e. measured with an empty cell) capacity C_0 and substrate capacity C_{su} through the measurement of a standard material with known permittivity (mineral B-oil, Vacuubrand). Assuming that the electric field penetrates only in the sample and the substrate, the measured capacity C_m^* is given by [44]:

$$C_m^* = C_0(\varepsilon_s^* + \varepsilon_{su}^*) \quad (1)$$

Where ε_s^* and ε_{su}^* are the complex permittivity of the sample and the substrate, respectively. The measurements were carried out in a frequency range of $2{\cdot}10^6$ Hz to 0.1 Hz with an Alpha Analyzer (Novocontrol Technologies) allowing measurement of the complex impedance as a function of frequency. The dielectric spectra were collected over a wide temperature range (from −150 to 150 °C) with appropriate successive steps. Accurate temperature control was implemented using the Quatro system (Novocontrol Technologies) allowing a temperature stability of ± 0.2 °C. During the measurement, the sample was kept in a nitrogen atmosphere. The dielectric relaxation curves were analyzed using the Havriliak-Negami (HN) complex function [45, 46]:

$$\varepsilon^* = \varepsilon_\infty + \frac{\Delta\varepsilon_{HN}}{[1+(i\omega\tau_{HN})^{\alpha_{HN}}]^{\beta_{HN}}} \quad (2)$$

This formalism allows fitting the real and imaginary components of the complex dielectric permittivity $\varepsilon^*(\omega)$ with three equations expressing $\varepsilon'(\omega)$, $\varepsilon"(\omega)$ and φ_{HN} as a function of the angular position $\omega = 2\pi f$, the relaxation strength $\Delta\varepsilon_{HN}$, the relaxation time τ_{HN}, and two parameters representing the broadening and asymmetric shape factors of the fitting curve α_{HN} and β_{HN}, respectively.

The side-effects due to conductivity were treated by adding a contribution $\varepsilon"_{cond} = \sigma_0/(\omega^s \varepsilon_0)$ to the dielectric loss, where σ_0 is the DC conductivity of the sample accounting for the Ohmic conduction related to the mobile charge carriers, *s* is a fitting parameter and ε_0 is the dielectric permittivity of vacuum.

Thermo-stimulated depolarization current (TSDC). TSDC experiments were performed using interdigitated electrodes placed into the cell containing the sample, and using the 6517B electrometer/high resistance meter (Keithley) provided by Novocontrol Technologies. IE calibration was performed as previously described for DRS experiments. The temperature control was ensured by a flow of heated (or cooled) gaseous nitrogen through the Quatro system (Novocontrol Technologies). Each sample was first heated up to a temperature a few degrees above the calorimetric glass transition temperature ($T_{g\ MT\text{-}DSC}$ + 5 °C) with the aim of erasing any previous thermal history. Then a protocol was run to select the optimal polarization temperature, i.e. the sample was polarized with a direct electric field of 1.10^5 V/m during a polarization time $t_{pol} = 5$ min while being heated from 2 °C below, to an increasingly higher temperature (up to 10 °C above $Tg_{\ MT\text{-}DSC}$) with a step of 2 °C, and then rapidly cooled to 0 °C while keeping the applied electric field. The depolarization current was recorded during the subsequent heating ramps from 0 °C to 110 °C at a rate of 5 K/min. This procedure allowed to select the polarization temperature ($Tg_{\ MT\text{-}DSC}$ + 6 °C) providing the best compromise between instability/decay phenomena (observed when the polarization temperature is too high) and low signal-to-noise ratio (observed when the polarization temperature is too low). The optimization of the polarization temperature allowed to obtain well-defined non-partial polarization peaks, with minimized parasite signals such as conductivity.

TSDC measurements could be used to analyze the segmental relaxation with the Kohlrausch-Williams-Watts (KWW) formalism, as proposed by Alegría et al. [47]. The relaxation time associated with the segmental relaxation was calculated as [48]:

$$\tau = \beta_{KWW} \frac{Q}{I} \left[ln \frac{Q_0}{Q} \right]^{1-\frac{1}{\beta_{KWW}}} \quad (3)$$

Where $Q(t) = \int_t^\infty Idt$ is the charge calculated as a function of time, Q_0 is the charge stored during the initial polarization process and prior to measurement, I is the current intensity, and β_{KWW} is a parameter considering the non-Debye character of segmental relaxation obtained by DRS. Alegría et al. underlined that the relaxation phenomena measured below T_g are affected by physical ageing; however, they also reported that physical ageing has a weak effect on the β_{KWW} parameter.

Results and discussion

Amplitude of cooperative motions at the glass transition.

Fig. 1 shows the *C'* signals measured by MT-DSC as a function of temperature in the range of the glass transition, which appears as an endothermic step. The derivative of *C'* with respect to temperature (dC'/dT) reveals a peak, whose maximum corresponds to the inflection of the heat capacity step, and is related to the dynamic glass transition temperature T_α characteristic of the selected oscillating parameters. These curves were used to determine T_α and measure the heat capacity step at its inflection ΔC_p (T_α), which are the main features of glass transition.

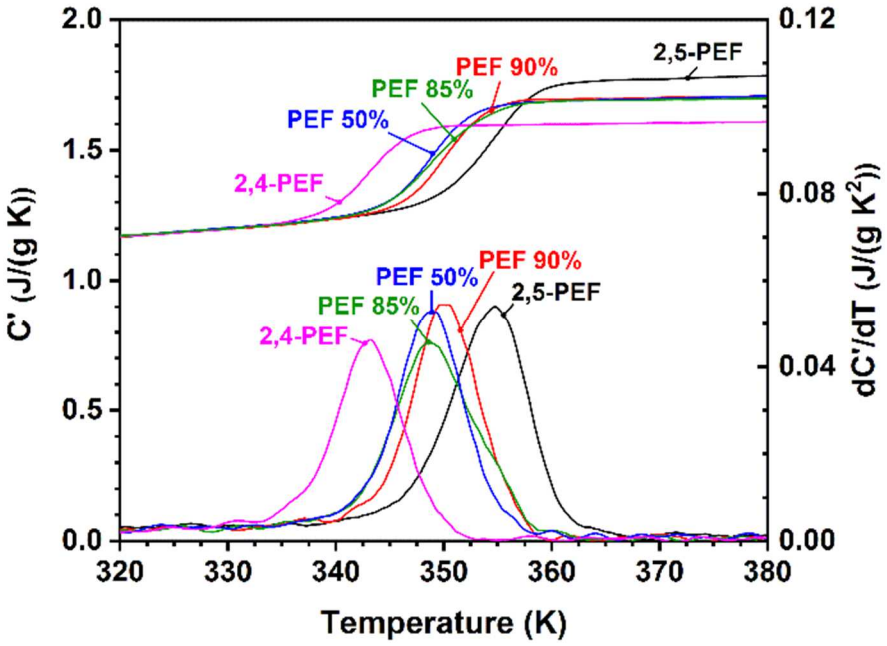

Figure 1. Temperature dependence of the real component of the apparent heat capacity (C') recorded by MT-DSC, and its derivative with respect to temperature (dC'/dT).

The average number of units relaxing in a CRR (N_α) and the average scale of a CRR, also called the cooperativity length (ξ_α), can be estimated on the basis of MT-DSC measurements according to Donth's method [39], which assumes that the mean temperature fluctuation δT within each CRR is associated with the standard deviation of the Gaussian function fitting the peak obtained at the glass transition. The equations to calculate ξ_α and N_α are the following:

$$\xi_\alpha^3 = \frac{\left(\frac{1}{C_{p\ glass}(T\alpha)} - \frac{1}{C_{p\ liquid}(T\alpha)}\right) k_B T_\alpha^2}{\rho(\delta T)^2} \quad (4)$$

$$N_\alpha = \frac{\rho N_A \xi_\alpha^3}{M_0} \quad (5)$$

Where C_p is the specific heat capacity at constant pressure and $C_{p\ glass}(T_\alpha)$ and $C_{p\ liquid}(T_\alpha)$ are the values extrapolated from the glassy and the liquid states to the dynamic glass transition temperature, k_B is Boltzmann's constant, ρ is the density, δT is obtained from the Full Width Half Maximum parameter of the Gaussian fit ($FWHM/2.355$), N_A is the Avogadro number and M_0 is the molar mass of the repeating unit. More details about the calculation of δT, N_α

and ξ_α from MT-DSC curves can be found in the work by Saiter et al. [40]. The results obtained with the curves shown in Fig. 1 are reported in Table 2.

Table 2. Heat capacity step at the dynamic glass transition (ΔC_p (T_α)), dynamic glass transition estimated by MT-DSC ($T_{\alpha\,MT\text{-}DSC}$) as the maximum of the peak in the *C'* derivative signal, cooperativity length (ξ_α) and number of equivalent relaxation units in a CRR (N_α) obtained from MT-DSC curves according to Donth's approach [39, 40].

	ΔC_p (T_α) (J/(g K))	$T_{\alpha\,MT\text{-}DSC}$ (°C)	ξ_α (nm)	N_α
2,5-PEF	0.46 ± 0.09	81 ± 2	2.8 ± 0.2	99 ± 10
PE-2,5[90]-2,4[10]F	0.42 ± 0.04	77 ± 2	2.9 ± 0.2	118 ± 10
PE-2,5[85]-2,4[15]F	0.42 ± 0.09	76 ± 3	2.6 ± 0.3	81 ± 15
PE-2,5[50]-2,4[50]F	0.43 ± 0.01	76 ± 2	3.0 ± 0.2	128 ± 10
2,4-PEF	0.33 ± 0.04	70 ± 1	2.9 ± 0.2	119 ± 10

Consistently with the values of glass transition temperature measured by conventional DSC for the homopolymers [31], T_α is about 10 °C higher for 2,5-PEF as compared to 2,4-PEF. This difference has been attributed to molecular mobility, itself associated with the different position of the carbonyl groups on the furan ring. Indeed, 2,5-FDCA (in 2,5-PEF) is symmetric but less linear than benzene (in PET), whereas 2,4-FDCA (in 2,4-PEF) is neither linear nor symmetric. Non-linearity affects the ring-flipping energy barrier [19], thus a restriction of the ring-flipping process should also be expected as a consequence of asymmetry; a reduction in chain segment mobility for 2,5-PEF resulting from the hindrance of furan ring flipping has been reported in the literature compared to the benzene ring contained in PET [19, 41, 49]. The MT-DSC curves of the 2,5/2,4-PEF copolymers (Fig. 1) are all characterized by a single endothermic step and values of T_α that are close to each other and intermediate with respect to the values obtained for the homopolymers. These results are

consistent with the values obtained by conventional DSC in a previous work [30]. The average CRR volume and number of relaxing units were calculated assuming that the amorphous phase has a density ρ = 1.434 g/cm^3 [18] and considering that the repeating unit has a molar mass M_0 = 182.14 g/mol. For comparison's sake, the same values of ρ and M_0 were used for all the samples. The cooperativity length ξ_α obtained for 2,5-PEF from MT-DSC measurements is in agreement with the value of 2.9 nm previously reported by Codou et al. [41]. All the polymers investigated in this work, independently on their composition, have similar CCR sizes and numbers of equivalent relaxation units in the CRR at the glass transition temperature. The literature reports examples where the CRR size is modified by geometric restrictions, such as the presence of crystalline lamellae [50], or as a consequence of processing techniques creating multi-nanolayers films [37]. However, when the amorphous domains are unconfined and can reasonably be considered as isotropic, a value of ξ_α = 3 nm is generally expected at T_α [39, 43, 51]. The results reported here make no exception, and show that whatever the composition, and in particular the ratio of position isomers in the backbone, the two homopolymers and the three copolymers have similar cooperativity at the glass transition.

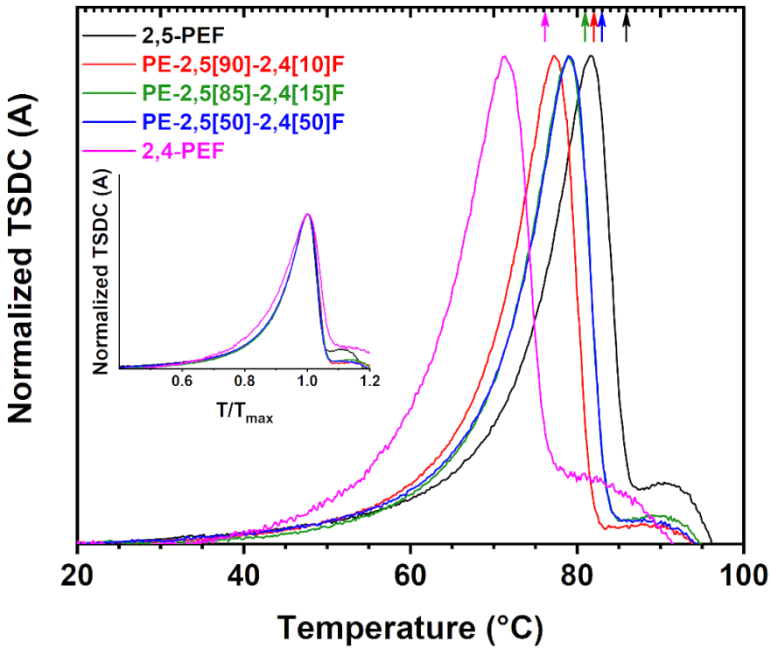

Figure 2. Normalized depolarization currents as a function of temperature measured by TSDC while heating from the glassy to the rubbery state. The arrows correspond to the temperature at which each sample was polarized prior to measurement. Inset: depolarization peaks normalized to the temperature of their maximum.

Fig. 2 shows the dielectric manifestation of the glass transition on TSDC measurements. The depolarization currents, recorded while heating the samples from the glassy to the rubbery state, are represented as a function of temperature. The temperature corresponding to the maximum of the depolarization peak ($T\alpha_{TSDC}$) is the highest for 2,5-PEF and shifts towards lower temperatures as the content of 2,4-FDCA-based repeating units increases. The values obtained by TSDC are in good agreement with the glass transition temperatures measured by DSC, as generally reported in the literature for other polymers [52-54]. The insert to Fig. 2 shows that, beside the temperature shift, the shape of the depolarization peaks is similar for all the samples, suggesting similar distributions of the relaxation times for segmental relaxation. This distribution is also related to cooperativity [55-57], therefore similar shapes of the depolarization peaks correlate well with the relative invariance of the cooperativity parameters (N_α and ξ_α) obtained by MT-DSC (Table 2).

Molecular mobility evaluated by DRS.

Fig. 3 shows an example of 3D plot of the imaginary component of the complex permittivity recorded as a function of temperature and frequency. In particular, the data in Fig. 3 were recorded for the 2,5/2,4-PEF copolymer containing 50:50 mol % of the two isomers (PE-2,5[50]-2,4[50]F), and illustrate the frequency and temperature dependences of the structural α relaxation and of the local β relaxations. A wide β relaxation is observed across the 3D plot, along with a narrower and more intense α relaxation at higher temperatures. A dramatic increase in the loss factor (ε") is observed at the highest temperatures and lowest frequencies, which is a common manifestation of conductivity phenomena.

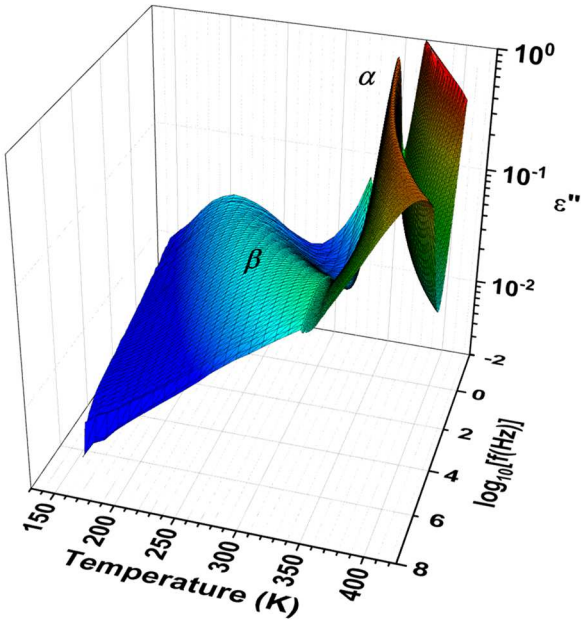

Figure 3. Example of 3D plot obtained by DRS for the 2,5/2,4-PEF copolymer containing 50:50 mol % of the two FDCA-based isomers (PE-2,5[50]-2,4[50]F). The dielectric loss (ε") is represented as a function of frequency (f) and temperature (T).

DRS measurements previously performed on the two homopolymers revealed two relaxation processes (α and β) for both 2,5-PEF and 2,4-PEF, the first one (β relaxation) recorded at low temperature and frequency, and the second one (α relaxation) located at higher temperature and well separated from the β relaxation [31]. The position and shape of these two relaxation

processes allowed to fit the experimental data with the sum of two HN functions, plus a contribution taking into account the conductivity phenomena building up at the highest temperatures and lowest frequencies, as illustrated in Fig. 4-a. This analytical approach revealed that the position isomerism due to a different connection of the carbonyl groups to the furan ring mostly affected the local β relaxation processes; localized molecular movements required shorter relaxation times in the symmetrical 2,5-PEF with respect to its asymmetrical counterpart 2,4-PEF. There are works in the literature suggesting to fit the experimental data for the β relaxation processes in polyesters with more than a single HN function; Soccio et al. [58], for instance, who investigated the local and segmental relaxation dynamics of poly(butylene 2,5-furanoate) (PBF), reported that local dynamics are associated with a broad relaxation that can be described by two processes, respectively related to the more mobile (glycolic) subunit and to the stiffer (acidic) moiety. This approach has been used to describe the relaxation phenomena in other polyesters in comparison with PET [59, 60], as well as in different polymers such as bisphenol A polycarbonate [61]. Considering that the main difference between 2,5-PEF and 2,4-PEF was detected by Bourdet et al. [31] on the local β relaxations, and that the samples in this study have a repeating unit with dipoles associated either to the furan ring (acidic moiety, expected to be less mobile) or to the glycolic subunit (expected to be more mobile) [58], all the DRS analyses were performed by fitting the experimental data with three HN functions (α, β_2 and β_1) plus a contribution accounting for conductivity, as illustrated in Fig. 4-a plus Fig. 4-b. The need for two HN contributions to describe the local β relaxation movements is particularly visible at low temperature and high frequency, both in the homopolymers and the copolymers, as shown by the example provided in Fig. 4-b. This probably explains the choice of some authors to use a single HN function for local β relaxations. Papamokos et al. [62], for instance, who investigated chain conformation, molecular dynamics and thermal properties of poly(*n*-methylene 2,5-furanoates) as a function

of methylene unit sequence length, did not consider the possibility of having two β relaxations because the analysis was not performed at low temperatures. Genovese et al. [63] investigated the effect of the chemical structure on the sub-glass relaxation dynamics of biobased polyesters by DRS, and compared 2,5-FDCA with trans-1,4-cyclohexanedicarboxylic acid; for the β relaxation of the furan-based polyester they used a single HN function, but an additional HN function could have been used at higher frequencies.

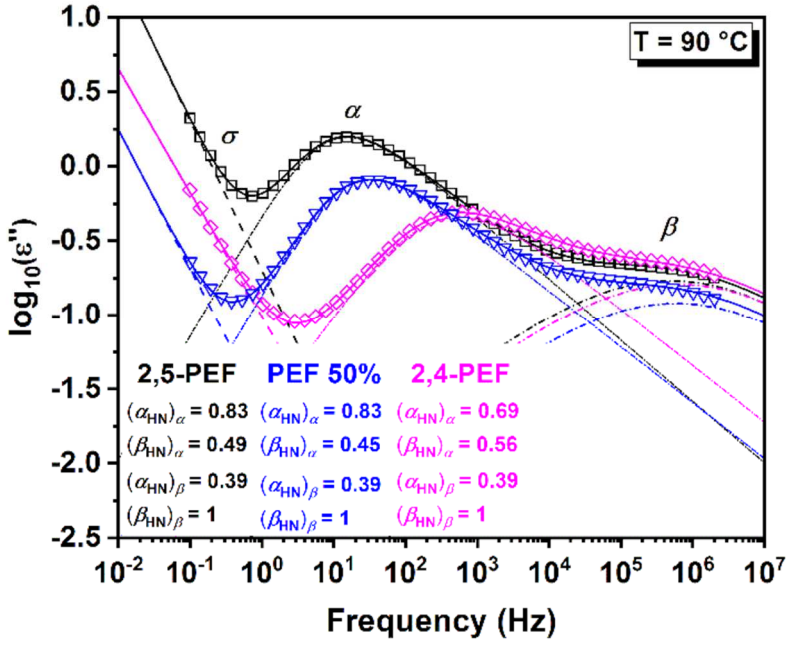

(a)

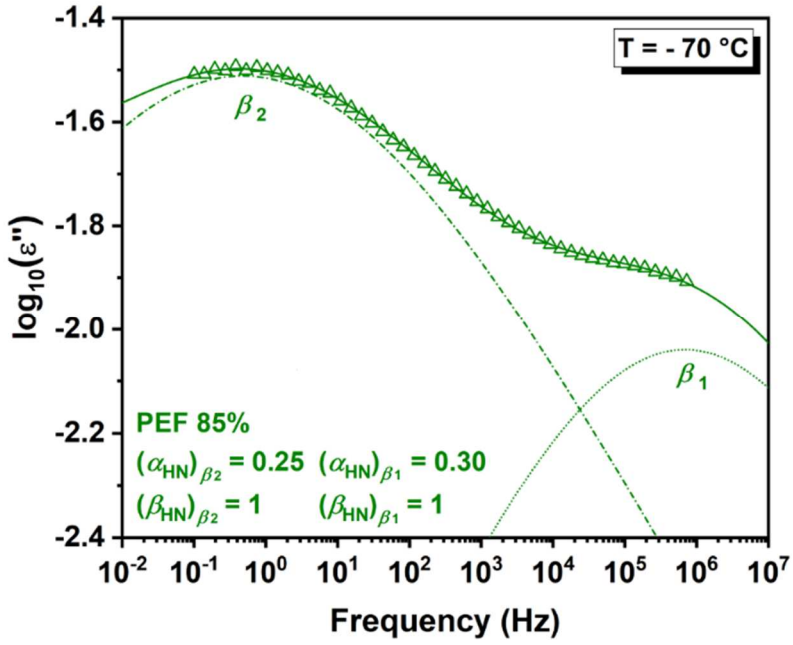

(b)

Figure 4. Illustration of the analytical procedure used to investigate the relaxation phenomena observed by DRS at (a) 90 °C and (b) -70 °C. Fitting included a contribution taking into account conductivity (σ), plus three Havriliak-Negami (HN) complex functions approaching the contributions from both the segmental and local relaxation phenomena (α, β_2 and β_1). The HN shape parameters for all the processes are also reported for each sample. The fitting procedure was applied to both the imaginary and real components of the complex ε^* signal in order to improve the accuracy of the resulting fitting parameters.

In this work, the analytical approach generally used for a simple HN relaxation phenomenon was extended to a larger temperature range and included both the peaks representing the β_2 and β_1 relaxation phenomena; the relaxation times associated with each contribution ($\tau_{max_{\beta_2}}$ and $\tau_{max_{\beta_1}}$) were plotted as a function of temperature, providing the relaxation maps reported in Fig. 5-a. The trends obtained for the β_2 and β_1 relaxation processes are in good agreement with the Arrhenius law and could be fitted with the following equation:

$$\tau = \tau_{0,A}\exp\left(\frac{E_a}{RT}\right) \quad (6)$$

Where E_a is the activation energy of the relaxation process, R is the gas constant, and $\tau_{0,A}$ is a pre-exponential factor.

The association of 2,4- and 2,5-FDCA during the synthesis of the copolymers has consequences on the β relaxation, for the time required by the local relaxation movements generally increases with the amount of 2,4-FDCA-based repeating units introduced in the backbone. Considering the different bond angles and structural arrangements in the 2,5- and 2,4-FDCA isomers [29], and since at each temperature the lowest value of relaxation time is obtained for the homopolymer 2,5-PEF as reported in the literature [31], it is reasonable to assume that this dependence is mainly related to the difference in linearity and symmetry between the two position isomers.

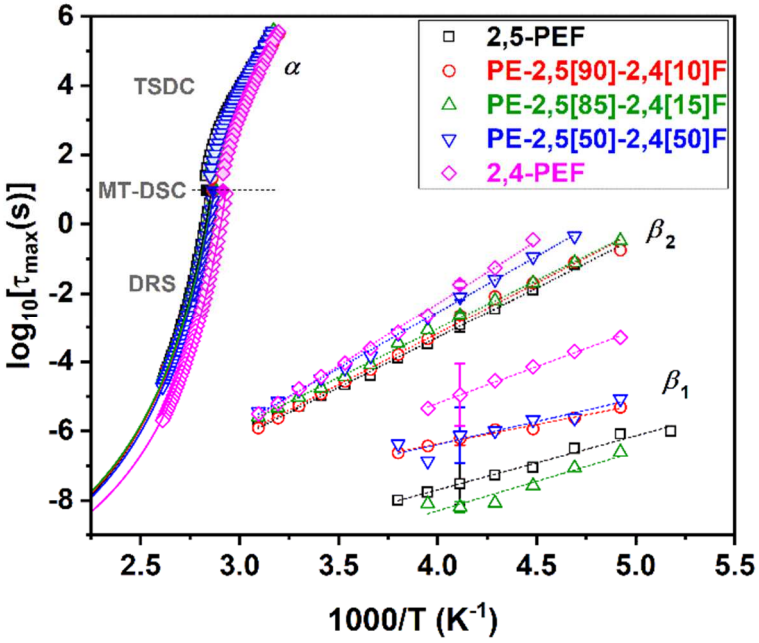

(a)

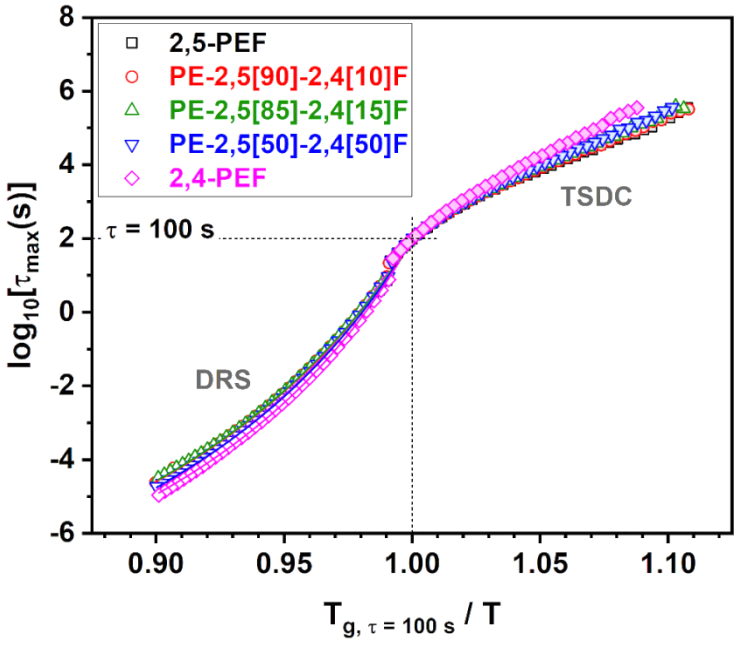

(b)

Figure 5. (a) Relaxation maps providing the temperature dependence of the relaxation time for both the segmental α relaxation and the local β relaxation processes, resolved with two HN functions associated to two relaxation phenomena (β_2 et β_1). Uncertainties are represented by error bars on the data at 1000/T = 4.1 K^{-1} (b) Extended Angell's plots obtained by DRS at temperatures above the glass transition and TSDC at temperatures below the glass transition. The logarithmic values of the relaxation times obtained with the HN fitting procedure $log_{10}(\tau_{HN})$ are represented as a function of the inverse temperature normalized to the glass transition temperature T_g/T.

Indeed, the higher is the number of non-linear and strongly asymmetrical 2,4-FDCA-based repeating units in the backbone, the more disordered is expected to be the conformation of the macromolecules in the entangled random coils [64], and the longer the time required for the local relaxation movements at any given temperature. This trend makes sense when compared to the reduced possibility for the furan rings to flip because of the non-linearity of the ring rotation axis with respect to the benzene ring [19, 41, 49]. This effect is slightly enlightened by a decrease in temperature, probably because of the temperature dependence of density and free volume, which brings the molecules together as thermal agitation decreases and reinforce the hindrance effect on mobility.

Activation energy associated with the local relaxation movements.

Table 3 reports the values of activation energy for each HN contribution to the local relaxation movements, $E_a(\beta_2)$ and $E_a(\beta_1)$, calculated with Eq. 6. The values of $E_a(\beta_2)$ obtained in this work are not so different from the activation energies previously obtained with a single HN function for the homopolymers 2,5-PEF and 2,4-PEF (56 and 75 kJ·mol^{-1}, respectively) [31]; they are also not so different from the values reported in the literature for other polyesters, usually associated to the local motions of the ester groups (36 kJ·mol^{-1} for polylactic acid (PLA) [65], 55 kJ·mol^{-1} for poly (hydroxybutyrate-*co*-hydroxyvalerate) (PHBV) [66], 79 kJ·mol^{-1} for polyethylene terephthalate (PET) [59]). Interestingly, the activation energy for the local β relaxation is higher for cyclic polyesters (PET) as compared to linear polyesters (PHBV and PLA). Soccio et al. [58] explored the local relaxation phenomena in poly (butylene 2,5-furanoate) by fitting the DRS data with a double HN contribution, one related to the dipole directly connected to the furan ring (acidic moiety, with slower molecular mobility), the other related to the dipole bringing together the acidic moiety to the glycolic subunit (which is the most flexible segment of the backbone, with the fastest molecular mobility).

Table 3. Summary of the values obtained by DRS and TSDC: $T_{g_{\tau=100s}}$ and $T_{g_{\tau=10s}}$ are the glass transition temperatures for $\tau = 100$ s and $\tau = 10$ s, D is a dimensionless parameter required by the VTF fitting and T_0 is Vogel temperature (as specified in Eq. 7), $\tau_{0,\alpha}$ is the relaxation time extrapolated at an infinite temperature, m_{liquid} is the fragility index calculated by DRS, $\tau_{0,A\beta_2}$ and $\tau_{0,A\beta_1}$ are the pre-exponential factors in the Arrhenius law, $E_a(\beta_2)$ and $E_a(\beta_1)$ are the values of activation energy obtained by fitting the local relaxation movements with two HN contributions, T_α is the glass transition temperature and m_{glass} is the fragility index calculated by TSDC.

	DRS										TSDC	
	$T_{g_{\tau=100s}}$ (°C)	$T_{g_{\tau=10s}}$ (°C)	D	T_0 (°C)	$log_{10}(\tau_{0,\alpha})$ (s)	m_{liquid}	$log_{10}(\tau_{0,A\beta_2})$ (s)	$E_a(\beta_2)$ (kJ·mol^{-1})	$log_{10}(\tau_{0,A\beta_1})$ (s)	$E_a(\beta_1)$ (kJ·mol^{-1})	T_α (°C)	m_{glass}
2,5-PEF	74 ± 1	77 ± 1	4.42	31	-12	117 ± 10	-15	56 ± 6	-15	30 ± 10	82 ± 1	82 ± 10
2,5/2,4-PEF 90%	72 ± 1	75 ± 1	4.64	29	-12	112 ± 10	-14	57 ± 6	-16	22 ± 10	77 ± 1	78 ± 10
2,5/2,4-PEF 85%	72 ± 1	75 ± 1	4.67	29	-12	112 ± 10	-15	55 ± 6	-12	33 ± 10	79 ± 1	80 ± 10
2,5/2,4-PEF 50%	72 ± 1	75 ± 1	4.40	31	-12	118 ± 10	-11	65 ± 6	-17	25 ± 10	79 ± 1	83 ± 10
2,4-PEF	65 ± 1	68 ± 1	4.10	27	-12	125 ± 10	-14	72 ± 6	-14	41 ± 10	71 ± 1	85 ± 10

In this work, the β_2 relaxation seems to better represent the association of 2,4- and 2,5-FDCA for the synthesis of 2,5/2,4-PEF copolymers, for the corresponding activation energy $E_a(\beta_2)$ follows a sort of mixing rule (as shown by the activation energy of the PE-2,5[50]-2,4[50]F copolymer, which is average between the values obtained for the homopolymers). The β_1 relaxation phenomenon seems to be less representative of the reduction in molecular mobility induced by the position isomerism of the carbonyl groups on the furan ring, for the corresponding activation energy $E_a(\beta_1)$ varies significantly with the isomer ratio but does not follow any predictive rule. These results can probably be explained by the fact that position isomerism is bear by the furan ring, and the slowest local movements are likely to be associated to the ring-flipping mechanism; indeed, the rotation of the C-C bonds linking the carbonyl groups to the furan rings are hindered proportionally to the content of the non-linear and asymmetric 2,4-FDCA-based repeating units. Besides, the dipole associated with the C-O bond between the carbonyl group and the glycolic subunit is smaller than the dipole represented by the carbonyl group itself, as well as farer from the molecular site determining the position isomerism, and therefore less affected. This interpretation is supported by results previously reported in the literature by Burgess et al. [19] who compared 2,5-PEF and PET, and Mackintosh et al. [59] who beforehand investigated poly(trimethylene terephthalate) (PTT) as compared to poly(ethylene terephthalate) (PET) and poly(ethylene naphtalate) (PEN), about the dependence of ring-flipping on the chemistry as well as on the symmetry of the connections to the polymer backbone. Nolasco et al. [64] recently confirmed the regiochemistry preferences of 2,4-FDCA-based repeating units to form randomly coiled chains based on *gauche*-ethylene glycol segments. It is also worth pointing out that the β_1 relaxation is identified in a low-intensity signal, observed through the movements of a relatively small dipole; this is an additional difficulty for measurement and fitting, and the results are therefore affected by large uncertainties. Besides, if the dipole responsible for the

β_1 relaxation process corresponds to the C-O bond linking the carbonyl group to the glycolic subunit, which is formed during the polymerization of FDCA with ethylene glycol, it would be reasonable to presume that the β_1 relaxation is the most sensitive to any possible composition heterogeneity affecting samples synthesized in small batches, especially when the isomer ratio is supposed to be finely tuned. This may be the case of PE-2,5[85]-2,4[15]F, whose β_1 relaxation falls out of the trend established by the other samples.

Fragility index in the liquid and glassy states.

Besides the effects on the local β relaxations, Fig. 5-a shows that the α relaxation is clearly modified by the incorporation of 2,4-FDCA-based repeating units in the polymer backbone. This result is consistent with the conclusions previously drawn by Soccio et al. [58] about poly (butylene 2,5-furanoate), asserting that fragility (a feature inherent to the α relaxation) is mainly correlated to the acidic moiety. Unsurprisingly, in this case the subunit that bears the carboxylic acid responsible for position isomerim is the acidic moiety, i.e. the furan ring. The relaxation maps in Fig. 5-a shows that the α relaxation for 2,5-PEF appears at higher temperature with respect to 2,4-PEF, and that the copolymers are closer to 2,5-PEF rather than to 2,4-PEF. The temperature dependence of the relaxation time obtained from the HN fitting for the α relaxation process follows the expected Vogel-Tamman-Fulcher (VTF) dependence [67-69]:

$$\tau = \tau_0 \exp\left(\frac{DT_0}{T-T_0}\right) \quad (7)$$

Where D corresponds to a fragility strength and T_0 is Vogel temperature.

Using the VTF parameters, a value of dielectric glass transition temperature can be calculated for a relaxation time equal to 100s and 10s (it has been proven the latter better corresponds to the experimental conditions used for MT-DSC experiments) [70] (Table 3). The values obtained by DRS for the copolymers are almost identical, regardless the ratio of 2,5/2,4-FDCA. In general, the values of glass transition temperature obtained by DRS are in good

agreement with the results obtained by other thermal techniques, such as DSC or MT-DSC [37, 71]. The main advantage of DRS with respect to DSC and MT-DSC is the measurement of different values of T_g in a wider range of frequencies, i.e. for different relaxation times, which makes it possible to investigate the molecular dynamics of the glass-forming liquid as it approaches the glass transition upon cooling. The fragility index m was introduced by Angell [72] on the basis of the homonymous plot in order to classify glass-formers using the temperature dependence of the relaxation times associated with their structural α relaxation, as expressed by Eq. 8:

$$m = \left.\frac{d log_{10}(\tau)}{d(T_g/T)}\right|_{T=T_g} \tag{8}$$

Small values of the fragility index are representative of an Arrhenius-like behavior, i.e. a linear dependence of the logarithmic values of the relaxation times $log_{10}(\tau)$ (extracted from the maximum of the peak in each HN function) as a function of the inverse temperature normalized to the glass transition temperature T_g/T. Such a behavior is typical of "strong" supercooled liquids. The more the dependence of $log_{10}(\tau_{HN})$ vs. T_g/T deviates from linearity, the more "fragile" is the glass-forming liquid. Kunal et al. [32] correlated fragility with a loss in packing efficiency, that is why polymers (with large steric hindrance due to the long macromolecular chains) are generally classified as fragile glass formers, whereas smaller molecules (such as pharmaceutical molecules [73, 74]) are generally classified as stronger glass formers. The m value is typically calculated from the temperature dependence of the relaxation time in the liquid state (i.e. in the temperature range just above the glass transition, as temperature decreases until reaching the value of $T_{g_{\tau=100s}}$) by DRS; the same calculation can also be done from the temperature dependence of the relaxation time in the glassy state (i.e. in the temperature range just below the glass transition, as temperature increases until reaching $T_{g_{\tau=100s}}$) by TSDC [57, 75]. The Angell's plot [72] obtained with DRS data, and

then extended to a temperature range below the glass transition thanks to TSDC, is reported in Fig. 5-b. The different sets of experimental data overlap well in the glass transition region, meaning that the temperature dependences of the relaxation time obtained by the two techniques are in good agreement with each other. At temperatures far below the glass transition (i.e. at the extreme right side of TSDC curves), the temperature dependence of the relaxation time is Arrhenius-like, then it gradually deviates from linearity as the temperature increases and approaches the glass transition. The steepness of such deviation is representative of the progressive change in the activation energy associated with the structural α relaxation. The reverse behavior (i.e. the return to an Arrhenius-like behavior) is expected at temperatures far above the glass transition, and generally occurs in a temperature region that DRS measurements cannot cover. A thorough investigation of the relaxation phenomena in the sub-glass-transition temperature range is of uppermost importance and may be used, for instance, to investigate the aging processes as a function of different parameters, including position isomerism and the arrangement of different repeating units in copolymers, as announced for the model recently proposed by Ginzburg [42]. A difference in bond angles (PET vs. 2,5-PEF) [29], as well as an increased asymmetry due to position isomerism (2,5-PEF vs. 2,4-PEF), are expected to affect not only the regularity of the macromolecular conformations in the solid state [64] and the aptitude of the aromatic rings to flip [19], but also the relaxation dynamics. This observation may have significant consequences on physical ageing, occurring when non-equilibrium amorphous phases (e.g. polymers quenched from above the glass transition into the glassy state) approach an equilibrium state via small-scale relaxation processes [76]; it is widely held that both the α and β relaxation processes are engendered by local motions of the polymer backbone, and that there is a strong mechanistic connection between them, in the sense that the β relaxation process is a precursor for the cooperative α relaxation process [77]. The relaxation times plotted in Fig. 5-b were used to

calculate the fragility index both in the liquid state (m_{liquid}) and in the glassy state (m_{glass}) (Table 3). From DRS data, values of m_{liquid} of 117 and 125 were obtained for 2,5-PEF and 2,4-PEF, respectively; all the copolyesters provided values that are closer to 2,5-PEF rather than to 2,4-PEF. These values are consistent with the observations previously made by Bourdet et al. [31] on 2,5-PEF and 2,4-PEF, and confirm that the fragility of these polyesters is slightly lower with respect to other polymers (142 for PET [78], 144 for glycol-modified PET (PETg) [79], 170 for polycarbonate (PC) [80] and 150 for polylactic acid (PLA) [81]). The values of m_{glass} obtained from TSDC data are very similar to each other and close to 80 for all the samples (Table 3). In most polymers, the kinetic fragility index obtained from the glassy state by TSDC is lower than the one determined in the liquid-like state by DRS. Araujo et al. [57] recently reported that the difference in the two *m* values is an indicator of the cooperativity of the segmental relaxation. Obtaining similar *m* values regardless of the ratio of symmetric/asymmetric 2,5/2,4-FDCA isomers, suggests that position isomerism has no relevant effect on the temperature-induced curvature of the relaxation times associated with segmental relaxation. This result confirms that a minor modification of a few repeating units in a polymer backbone (in this case, the incorporation of small mol % of monomers whose chemistry is very similar to the main repeating units) is not enough to significantly affect the global behavior of the glass-forming liquid at the glass transition, unless it is accompanied by an extensive change in their chemistry, as observed by Soto Puente et al. [82] and later on by Varol et al. [83]. Apparently, a significant modification of the inter-chain interactions is generally required to make a difference in terms of fragility index. Such a modification can be achieved with a plasticizer, as shown by Araujo et al. [57, 84], but is most generally observed for systems having completely different chemical compositions, as reported by Kunal et al. [32]. Araujo et al. [85], for instance, recently reported an example of interpenetrated polymer networks based on acrylate (soft, flexible) and epoxy (stiff, rigid) systems, for which the

temperature dependence of the relaxation time depends on both the rigidity of the backbones and the intermolecular interactions.

Fluctuations of the intermolecular interactions.

The cooperativity of the segmental α relaxation introduced by Adam and Gibbs [33] is nowadays considered as a key parameter to characterize the fluctuations of intermolecular interactions in the amorphous phase as temperature decreases and the polymer goes from liquid to glassy. Several studies have tried to evidence the influence of different chemical compositions and macromolecular arrangements on the cooperativity length scale [37, 41, 51, 86]. The combination of MT-DSC and DRS allows access to the extended version of Donth's approach [39], providing the temperature dependence of cooperativity in a wider range of temperatures and frequencies [40]. Fig. 6 reports the values of the cooperativity length ξ_α as a function of the dynamic glass transition temperature T_α normalized to the calorimetric glass transition temperature. As expected, all the samples have a cooperativity length ξ_α that decreases with increasing temperature. No striking differences are observed in the values obtained by MT-DSC (filled symbols at $T_\alpha/T_g = 1$ in Fig. 6); however, a sort of trend emerges from the values obtained by DRS (hollow symbols in Fig. 6). The lowest cooperativity is obtained for both the homopolymers, with no significant difference due to position isomerism. The cooperativity of the copolymers is either equal to (as in the case of PE-2,5[90]-2,4[10]F) or slightly higher than (in the case of PE-2,5[85]-2,4[15]F and PE-2,5[50]-2,4[50]F) the cooperativity obtained for the homopolymers. Any polymer approaching the glass transition is known to exhibit dynamic heterogeneities, which means that fluctuations of the local relaxation times are observed from one point to another within the sample, with a characteristic length scale of a few nanometers. Dynamic heterogeneities are intrinsic to polymeric systems; they usually change as time goes by (during ageing) [87] and depend on external factors (e.g. pressure) [88], but are also affected by factors related to

chain connectivity, as well as spatial composition heterogeneities, which can be either intramolecular (as in the case of copolymers) or intermolecular (as in the case of polymer blends or plasticized polymers). The presence of composition fluctuations within volumes having similar sizes as the cooperatively rearranging regions can drive the effective local composition away from the mean, therefore affecting dynamic heterogeneities [89].

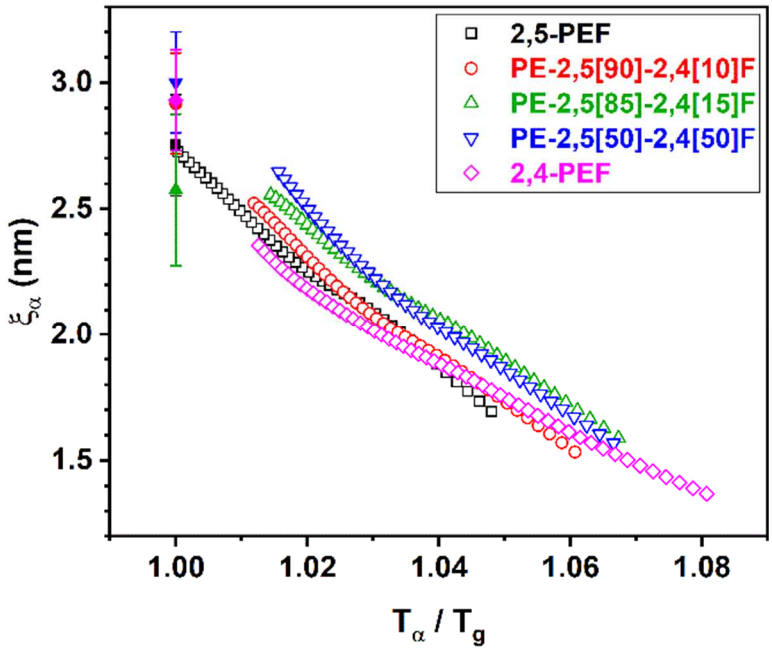

Figure 6. Cooperativity length ξ_α as a function of the dynamic glass transition temperature T_α normalized to the calorimetric glass transition temperature T_g. The values were calculated from DRS (hollow symbols) and MT-DSC (filled symbols) experimental data.

Fig. 6 seems to suggest that, besides being temperature-dependent, the cooperativity length (and therefore the CRR volume) also depends on the composition of the copolymers; this effect would be due neither to chemistry (because isomers have the same chemical composition and different atomic arrangements) nor to position isomerism (because 2,5-PEF and 2,4-PEF have the same cooperativity), but to the consequences of associating two isomeric repeating units in the same macromolecule.

In 2,5/2,4-PEF copolymers, composition fluctuations are expected to generate conformation fluctuations [64] (because the furan rings in the 2,5-FDCA-based repeating units and in the

2,4-FDCA-based repeating units have different abilities to flip) that are likely to drive density fluctuations; when these fluctuations occur within a length scale that is comparable to the cooperativity length, the consequences of copolymerization may eventually reinforce the dynamic heterogeneities intrinsically exhibited by each homopolymers. This may be surprising because in many cases, as for plasticized polymers [57] and polymer blends [83], composition fluctuations affect dynamic heterogeneities with mechanisms that increase (or reduce) free volume, and consequently reduce (or increase) cooperativity. It is however difficult to compare systems where the parameter affecting dynamic heterogeneities and cooperativity is interchain connectivity, with systems where composition heterogeneities are associated to intrachain connectivity. Besides, interchain connectivity is sometimes affected by intrachain connectivity, and 2,5/2,4-PEF copolymers could be an example. On the basis of the results recently reported by Nolasco et al. [64], the presence of 2,4-FDCA-based repeating units in a 2,5-FDCA-based polymer backbone would disrupt the formation of periodic interchain C–H···O contacts; this is how the authors explained the crystallization disruption observed in 2,4-PEF as compared to 2,5-PEF [29, 31]. The question regarding a possible structural origin of dynamic heterogeneities is still open; researchers keep on investigating different systems, including liquids under nanoconfinement [90] and interpenetrated polymer networks [85], to point out any possible mechanistic connection between the coexistence of strong spatial (e.g. composition) heterogeneities over length scales of a few nanometers, with structural and dynamic heterogeneities.

Activation energy associated with the segmental relaxation.

Besides measuring the kinetic fragility index and correlating it to cooperativity [57], Araujo et al. [84] investigated plasticized PLA also in terms of free volume and activation energy associated with the super-Arrhenius behavior typical of the segmental α relaxation, seeking a potential correlation. It is therefore interesting to plot the temperature dependence of the

activation energy required for the segmental α relaxation on the basis of both DRS and TSDC experimental data (i.e. as the glass transition is approached from the liquid and from the glassy states). The activation energy associated with the segmental α relaxation was calculated as [57]:

$$E_a = \frac{\partial \ln(\tau)}{\partial(1/T_\alpha)} R \quad (9)$$

Where τ is the relaxation time at T_α and R is the gas constant. Above T_g, the values of τ were obtained from DRS measurements using a VFT fitting law; below T_g, the values of τ were obtained from TSDC measurements smoothed with a 4th degree polynomial equation ($y = A_0 + A_1 x + A_2 x^2 + A_3 x^3 + A_4 x^4$) and then fitted according to the procedure reported by Alegría et al. [48]. As previously mentioned, the relaxation phenomena observed below T_g are affected by physical ageing and include ageing dynamics; for this reason, the activation energy measured below T_g (right-hand side of Fig. 7) does not correspond to the "intrinsic" (i.e. equilibrium) activation energy of the corresponding molecular processes.

The results are reported in Fig. 7 as a function of the inverse temperature normalized to the dynamic glass transition temperature T_α. The temperature dependences are very similar both in the liquid and in the glassy state for all the considered samples. The low-temperature Arrhenius behavior of the segmental α relaxation is clearly visible at the extreme right side of the plot, where the values of activation energy obtained by TSDC reach a plateau. The plots obtained from DRS data are clearly superimposed, whereas a slight difference is noticed in the TSDC plots for the two homopolymers (2,5-PEF and 2,4-PEF) and the copolymer with the lowest content of 2,4-FDCA-based repeating units (PE-2,5[90]-2,4[10]F) as compared to the copolymers having the highest potential for composition heterogeneities (PE-2,5[85]-2,4[15]F and PE-2,5[50]-2,4[50]F).

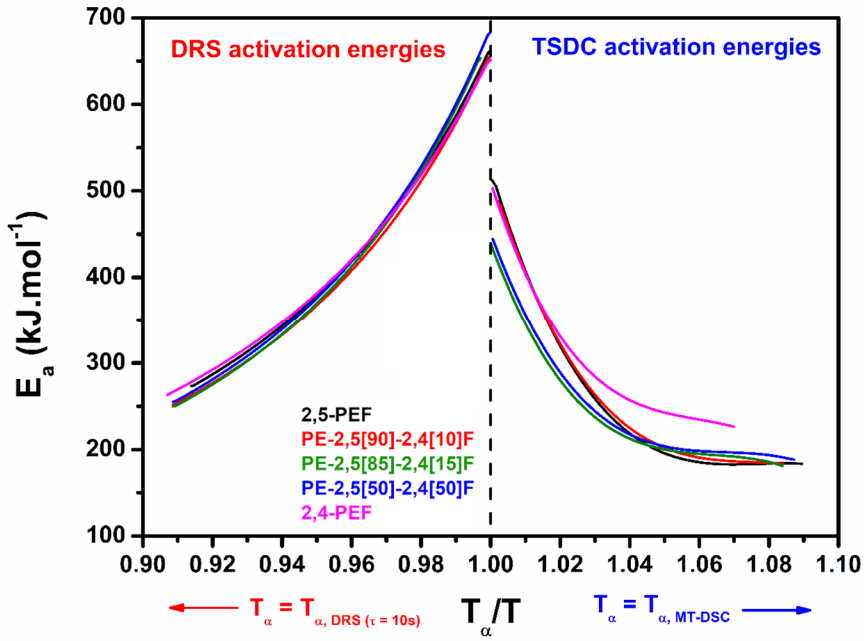

Figure 7. Activation energy required for the segmental α relaxation, calculated both from DRS and TSDC measurements, and plotted as a function of the inverse temperature normalized to the dynamic glass transition temperature T_α/T.

According to the results obtained by Araujo et al. [84] about plasticized PLA, lower values of activation energy would correlate with an increased amount of free volume, which is likely to be the case for 2,5/2,4-PEF copolymers, considering the possible fluctuation of molecular conformations due to position isomerism. However, a discrepancy appears when it comes to cooperativity. Araujo et al. [84] observed that cooperativity is maximum when free volume is minimum; they concluded that the amount of free volume in plasticized PLA is controlled by the amount of plasticizer in the composition, and that plasticization decreases both the fragility index and the scale of cooperative motions at the glass transition. In a later work [57] they observed that the CRR size decreases as the plasticizer content increases, and because the main consequence of plasticization lies in the decrease of interchain weak bonds, they assumed that interchain connectivity is the parameter driving the CRR size. The comparison of all the results reported so far encourages to draw a slightly different conclusion with respect to polymer blends or plasticized polymers. The incorporation of (asymmetrical) 2,4-

FDCA-based units into a polymer backbone mainly constituted of (symmetrical) 2,5-FDCA-based repeating units seems to be responsible for (1) longer relaxation times associated with the local β relaxation processes (Fig. 5) (the effect is proportional to the content of 2,4-FDCA-based repeating units and clearly depends on symmetry), (2) no striking effects of position isomerism on the kinetic fragility index (Table 3) with the expected difference in the values calculated from DRS (m_{liquid}) and from TSDC (m_{glass}), (3) no obvious effects on cooperativity (Fig. 6) even though a trend seems to emerge when the homopolymers and the copolymers are compared in the liquid state (the cooperativity length slightly increases when different repeating units are associated with respect to homopolymers), and (4) no effects on the activation energy for the segmental α relaxation in the liquid state (Fig. 7) but a decrease in the values of activation energy in the glassy state for the copolymers compared to the homopolymers (probably due to an increase in free volume). The literature proved, through different examples, that it is difficult to state whether dynamic heterogeneities are correlated to structural heterogeneities, and which is the relative importance of intramolecular and intermolecular chain connectivity (Van de Waals interaction, symmetry and ring-flipping, etc.) in molecular mobility and cooperativity. In such a complex scenario, the information obtained on the basis of the activation energy (both in the liquid and in the glassy state) appear to be as important as more conventional approaches based on the relaxation time and its temperature-dependence, the kinetic fragility index or the cooperativity length.

CONCLUSION

Furandicarboxylic acid (FDCA) exists in three forms differing by the position of the carbonyl groups on the furan ring (position isomers): 2,5-FDCA (obtained with the highest yield), 2,4-FDCA (so far considered as a by-product but obtained with yields that can be exploited), and 3,4-FDCA (traces). FDCA contains a five-membered aromatic ring with four carbon atoms and one oxygen, whereas terephthalic acid (TPA) contains a benzene ring with six carbon

atoms. Both rings are aromatic and have two substituents. The bond angles depend on the position of the substituents and determine the rotation axis of the ring. The ring-flipping mechanism is affected by the linearity of the rotation axis, as shown by the comparison of TPA with 2,5-FDCA. 2,5-FDCA and 2,4-FDCA are both less linear than TPA, with the difference that the position of the substituents is symmetric in 2,5-FDCA and strongly asymmetric in 2,4-FDCA. This work investigates the effects of position isomerism on the molecular mobility of a series of amorphous polyesters obtained by combining ethylene glycol (EG) with either 2,5-FDCA (homopolymer 2,5-PEF) or 2,4-FDCA (homopolymer 2,4-PEF), and also with different ratios of 2,5/2,4-FDCA (copolymers 2,5/2,4-PEF with 90:10, 85:15 and 50:50 mol %). The molecular mobility in the amorphous phase was investigated by cross-comparing the results obtained by Modulated-Temperature Differential Scanning Calorimetry (MT-DSC), Dielectric Relaxation Spectroscopy (DRS) and Thermo-Stimulated Depolarization Currents (TSDC). The relaxation times associated with both the local and segmental relaxation phenomena were measured over a large range of temperature and frequency. Due to the complexity of the relaxation phenomena, all the analyses were performed by fitting the experimental data with three Havriliak-Negami functions (α, $\beta 2$ and $\beta 1$) plus a contribution accounting for conductivity (σ). The temperature dependence of the relaxation time, the fragility index, the activation energy of each relaxation phenomenon, as well as the size of the cooperatively rearranging regions at the glass transition, were all investigated as the glass transition is approached both from the liquid (DRS) and from the glassy state (TSDC). The incorporation of 2,4-FDCA-based units into a polymer backbone mainly constituted of 2,5-FDCA-based repeating units is responsible for (i) a decrease in the glass transition temperature proportional to the isomer ratio, (ii) longer relaxation times associated with the local β relaxation processes, (iii) no striking effects on the fragility index, (iv) no obvious effects on cooperativity, but a slight increase in the size of the cooperatively

rearranging regions in the liquid state for the copolymers compared to the homopolymers, (v) no effects on the activation energy for the α relaxation in the liquid state, and (vi) a decrease in the activation energy for the α relaxation in the glassy state for the copolymers with the highest isomer ratios (85:15 and 50:50 mol %).

CRediT author statement

Aurélie Bourdet: polymer synthesis, MT-DSC and DRS investigations, data treatment and visualization, writing (initial draft) **Steven Araujo**: TSDC investigations, data treatment and visualization, critical review, commentary and revision of the final manuscript **Shanmugam Thiyagarajan**: polymer synthesis, supervision of sample selection and preparation **Laurent Delbreilh**: supervision of the investigations, validation of the research outputs, critical review, commentary and revision of the manuscript **Antonella Esposito**: coordination of the collaboration, supervision and validation of the investigations, writing, reviewing and editing **Eric Dargent**: funding acquisition, management of the research activity planning and execution, validation of the research outputs, critical review, commentary and revision of the manuscript

ACKNOWLEGMENTS

The authors thank the Normandie Region as well as the European Regional Development Fund for their financial support through the SCAMPI project. The authors also thank Clément Fosse for proof-reading the paper prior to submission.

REFERENCES

[1] Belgacem, M.; Gandini, A. Eds. *Monomers, Polymers and Composites from Renewable Resources*. 1st Edition. Elsevier, **2011**.

[2] Kalia, S.; Avérous, L. *Biodegradable and Biobased Polymers for Environmental and Biomedical Applications*. John Wiley & Sons, **2016**.

[3] Gandini, A.; Silvestre, A.J.D.; Neto, C.P.; Sousa A.F.; Gomes, M. The furan counterpart of poly(ethylene terephthalate): An alternative material based on renewable resources. *J. Pol. Sci. Part A: Pol. Chem.* **2009**, *47 (1)*, 295-298. https://doi.org/10.1002/pola.23130

[4] Sherman, L.M. *Coca-Cola Debuts First 100% Biobased PET Bottle* http://www.ptonline.com/blog/post/coca-cola-debuts-first-100-biobased-pet-bottle (accessed

June 15, 2017).

[5] Gandini, A.; Lacerda, T. M.; Carvalho, A. J. F.; Trovatti, E. Progress of Polymers from Renewable Resources: Furans, Vegetable Oils, and Polysaccharides. *Chem. Rev.* **2016**, *116 (3)*, 1637-1669. https://doi.org/10.1021/acs.chemrev.5b00264

[6] Sousa, A. F.; Matos, M.; Freire, C. S. R.; Silvestre, A. J. D.; Coelho, J. F. J. New Copolyesters Derived from Terephthalic and 2,5-Furandicarboxylic Acids: A Step Forward in the Development of Biobased Polyesters. *Polymer* **2013**, *54 (2)*, 513-519. https://doi.org/10.1016/j.polymer.2012.11.081

[7] de Jong, E.; Dam, M. A.; Sipos, L.; Gruter, G.-J. M. Furandicarboxylic Acid (FDCA), A Versatile Building Block for a Very Interesting Class of Polyesters. In *Biobased Monomers, Polymers, and Materials*; ACS Symposium Series. American Chemical Society, **2012**, *1105*, 1–13. https://doi.org/10.1021/bk-2012-1105.ch001

[8] Papageorgiou, G. Z.; Tsanaktsis, V.; Bikiaris, D. N. Synthesis of Poly(Ethylene Furandicarboxylate) Polyester Using Monomers Derived from Renewable Resources: Thermal Behavior Comparison with PET and PEN. *Phys. Chem. Chem. Phys.* **2014**, *16 (17)*, 7946-7958. https://doi.org/10.1039/C4CP00518J

[9] Lee, J.S.; Chandra, P.; Burgess, S.K.; Kriegel, R.; Koros, W.J. An advanced gas/vapor permeation system for barrier materials: Design and applications to poly(ethylene terephthalate). *J. Polym. Sci. B Polym. Phys.* **2012**, *50 (17)*, 1262-1270. https://doi.org/10.1002/polb.23116

[10] Burgess, S.K.; Karvan, O.; Johnson, J.R.; Kriegel, R.M.; Koros, W.J. Oxygen sorption and transport in amorphous poly(ethylene furanoate). *Polymer* **2014**, *55*, 4748-4756. https://doi.org/10.1016/j.polymer.2014.07.041

[11] Burgess, S.K.; Kriegel, R.M.; Koros, W.J. Carbon Dioxide Sorption and Transport in Amorphous Poly (ethylene furanoate). *Macromolecules* **2015**, *48 (7)*, 2184-2193. https://doi.org/10.1021/acs.macromol.5b00333

[12] Burgess, S.K.; Wenz, G.B.; Kriegel, R.M.; Koros, W.J. Penetrant transport in semicrystalline poly (ethylene furanoate). *Polymer* **2016**, *98*, 305-310. https://doi.org/10.1016/j.polymer.2016.06.046

[13] Stoclet, G.; Gobius du Sart, G.; Yeniad, B.; de Vos, S.; Lefebvre, J. M. Isothermal Crystallization and Structural Characterization of Poly(Ethylene-2,5-Furanoate). *Polymer* **2015**, *72*, 165-176. https://doi.org/10.1016/j.polymer.2015.07.014

[14] Mao, Y.; Bucknall, D. G.; Kriegel, R. M. Synchrotron X-Ray Scattering Study on Amorphous Poly(Ethylene Furanoate) under Uniaxial Deformation. *Polymer* **2018**, *139*, 60-

67. https://doi.org/10.1016/j.polymer.2018.01.062

[15] Mao, Y.; Bucknall, D. G.; Kriegel, R. M. Simultaneous WAXS/SAXS Study on Semi-Crystalline Poly(Ethylene Furanoate) under Uniaxial Stretching. *Polymer* **2018**, *143*, 228–236. https://doi.org/10.1016/j.polymer.2018.04.018

[16] Codou, A.; Guigo, N.; van Berkel, J.; de Jong, E.; Sbirrazzuoli, N. Non-Isothermal Crystallization Kinetics of Biobased Poly(Ethylene 2,5-Furandicarboxylate) Synthesized via the Direct Esterification Process. *Macromol. Chem. Phys.* **2014**, *215 (21)*, 2065-2074. https://doi.org/10.1002/macp.201400316

[17] Stoclet, G.; Lefebvre, J. M.; Yeniad, B.; Gobius du Sart, G.; de Vos, S. On the Strain-Induced Structural Evolution of Poly(Ethylene-2,5-Furanoate) upon Uniaxial Stretching: An in-Situ SAXS-WAXS Study. *Polymer* **2018**, *134*, 227-241. https://doi.org/10.1016/j.polymer.2017.11.071

[18] van Berkel, J. G.; Guigo, N.; Kolstad, J. J.; Sipos, L.; Wang, B.; Dam, M. A.; Sbirrazzuoli, N. Isothermal Crystallization Kinetics of Poly (Ethylene 2,5-Furandicarboxylate). *Macromol. Mater. Eng.* **2015**, *300 (4)*, 466-474. https://doi.org/10.1002/mame.201400376

[19] Burgess, S.K.; Leisen, J.E.; Kraftschik, B.E.; Mubarak, C.R.; Kriegel, R.M.; Koros, W.J. Chain Mobility, Thermal, and Mechanical Properties of Poly(ethylene furanoate) Compared to Poly(ethylene terephthalate). *Macromolecules* **2014**, 47 (4), 1383-1391. https://doi.org/10.1021/ma5000199

[20] Araujo, C. F.; Nolasco, M. M.; Ribeiro-Claro, P. J. A.; Rudić, S.; Silvestre, A. J. D.; Vaz, P. D.; Sousa, A. F. Inside PEF: Chain Conformation and Dynamics in Crystalline and Amorphous Domains. *Macromolecules* **2018**, *51 (9)*, 3515-3526. https://doi.org/10.1021/acs.macromol.8b00192

[21] Konstantopoulou, M.; Terzopoulou, Z.; Nerantzaki, M.; Tsagkalias, J.; Achilias, D. S.; Bikiaris, D. N.; Exarhopoulos, S.; Papageorgiou, D. G.; Papageorgiou, G. Z. Poly(Ethylene Furanoate-Co-Ethylene Terephthalate) Biobased Copolymers: Synthesis, Thermal Properties and Cocrystallization Behavior. *Eur. Polym. J.* **2017**, *89*, 349–366. https://doi.org/10.1016/j.eurpolymj.2017.02.037

[22] Wang, X.; Wang, Q.; Liu, S.; Wang, G. Biobased Copolyesters: Synthesis, Structure, Thermal and Mechanical Properties of Poly(Ethylene 2,5-Furandicarboxylate-Co-Ethylene 1,4-Cyclohexanedicarboxylate). *Polym. Degrad. Stab.* **2018**, *154*, 96-102. https://doi.org/10.1016/j.polymdegradstab.2018.05.026

[23] Wang, J.; Liu, X.; Zhu, J.; Jiang, Y. Copolyesters Based on 2,5-Furandicarboxylic Acid

(FDCA): Effect of 2,2,4,4-Tetramethyl-1,3-Cyclobutanediol Units on Their Properties. *Polymers* **2017**, *9*, 305. https://doi.org/10.3390/polym9090305

[24] Matos, M.; Sousa, A. F.; Fonseca, A. C.; Freire, C. S. R.; Coelho, J. F. J.; Silvestre, A. J. D. A New Generation of Furanic Copolyesters with Enhanced Degradability: Poly(Ethylene 2,5-Furandicarboxylate)-Co-Poly(Lactic Acid) Copolyesters. *Macromol. Chem. Phys.* **2014**, *215 (22)*, 2175-2184. https://doi.org/10.1002/macp.201400175

[25] Papadopoulos, L.; Magaziotis, A.; Nerantzaki, M.; Terzopoulou, Z.; Papageorgiou, G. Z.; Bikiaris, D. N. Synthesis and Characterization of Novel Poly(Ethylene Furanoate-Co-Adipate) Random Copolyesters with Enhanced Biodegradability. *Polym. Degrad. Stab.* **2018**, *156*, 32-42. https://doi.org/10.1016/j.polymdegradstab.2018.08.002

[26] Jiang, M.; Liu, Q.; Zhang, Q.; Ye, C.; Zhou, G. A Series of Furan-Aromatic Polyesters Synthesized via Direct Esterification Method Based on Renewable Resources. *J. Polym. Sci. Part Polym. Chem.* **2012**, *50 (5)*, 1026-1036. https://doi.org/10.1002/pola.25859

[27] Terzopoulou, Z.; Papadopoulos, L.; Zamboulis, A.; Papageorgiou, D.G.; Papageorgiou, G.Z.; Bikiaris, D.N. Tuning the Properties of Furandicarboxylic Acid-Based Polyesters with Copolymerization: A Review. *Polymers* **2020**, *12*, 1209. https://doi:10.3390/polym12061209

[28] Thiyagarajan, S.; Pukin, A.; Haveren, J. van; Lutz, M.; Es, D. S. van. Concurrent Formation of Furan-2,5- and Furan-2,4-Dicarboxylic Acid : Unexpected Aspects of the Henkel Reaction. *RSC Adv.* **2013**, *3 (36)*, 15678-15686. https://doi.org/10.1039/C3RA42457J

[29] Thiyagarajan, S.; Vogelzang, W.; Knoop, R. J. I.; E. Frissen, A.; Haveren, J. van; Es, D. S. van. Biobased Furandicarboxylic Acids (FDCAs): Effects of Isomeric Substitution on Polyester Synthesis and Properties. *Green Chem.* **2014**, *16 (4)*, 1957-1966. https://doi.org/10.1039/C3GC42184H

[30] Thiyagarajan, S.; Meijlink, M. A.; Bourdet, A.; Vogelzang, W.; Knoop, R. J. I.; Esposito, A.; Dargent, E.; van Es, D. S.; van Haveren, J. Synthesis and Thermal Properties of Bio-Based Copolyesters from the Mixtures of 2,5- and 2,4-Furandicarboxylic Acid with Different Diols. *ACS Sustain. Chem. Eng.* **2019**, *7 (22)*, 18505-18516. https://doi.org/10.1021/acssuschemeng.9b04463

[31] Bourdet, A.; Esposito, A.; Thiyagarajan, S.; Delbreilh, L.; Affouard, F.; Knoop, R. J. I.; Dargent, E. Molecular Mobility in Amorphous Biobased Poly(Ethylene 2,5-Furandicarboxylate) and Poly(Ethylene 2,4-Furandicarboxylate). *Macromolecules* **2018**, *51 (5)*, 1937-1945. https://doi.org/10.1021/acs.macromol.8b00108

[32] Kunal, K.; Robertson, C. G.; Pawlus, S.; Hahn, S. F.; Sokolov, A. P. Role of Chemical Structure in Fragility of Polymers: A Qualitative Picture. *Macromolecules* **2008**, *41 (19)*, 7232-7238. https://doi.org/10.1021/ma801155c

[33] Adam, G.; Gibbs, J. H. On the Temperature Dependence of Cooperative Relaxation Properties in Glass-Forming Liquids. *J. Chem. Phys.* **1965**, *43 (1)*, 139-146. https://doi.org/10.1063/1.1696442

[34] Schick, C. Glass Transition under Confinement-What Can Be Learned from Calorimetry. *Eur. Phys. J. Spec. Top.* **2010**, *189 (1)*, 3-36. https://doi.org/10.1140/epjst/e2010-01307-y

[35] Saiter, A.; Couderc, H.; Grenet, J. Characterisation of Structural Relaxation Phenomena in Polymeric Materials from Thermal Analysis Investigations. *J. Therm. Anal. Calorim.* **2007**, *88 (2)*, 483-488. https://doi.org/10.1007/s10973-006-8117-x

[36] Lixon, C.; Delpouve, N.; Saiter, A.; Dargent, E.; Grohens, Y. Evidence of Cooperative Rearranging Region Size Anisotropy for Drawn PET. *Eur. Polym. J.* **2008**, *44 (11)*, 3377-3384. https://doi.org/10.1016/j.eurpolymj.2008.08.001

[37] Arabeche, K.; Delbreilh, L.; Adhikari, R.; Michler, G. H.; Hiltner, A.; Baer, E.; Saiter, J.-M. Study of the Cooperativity at the Glass Transition Temperature in PC/PMMA Multilayered Films: Influence of Thickness Reduction from Macro- to Nanoscale. *Polymer* **2012**, *53 (6)*, 1355-1361. https://doi.org/10.1016/j.polymer.2012.01.045

[38] Monnier, X.; Chevalier, L.; Esposito, A.; Fernandez-Ballester, L ; Saiter, A.; Dargent, E. Local and segmental motions of the mobile amorphous fraction in semi-crystalline polylactide crystallized under quiescent and flow-induced conditions. *Polymer* **2017**, *126*, 141-151. https://doi.org/10.1016/j.polymer.2017.08.021

[39] Donth, E. The Size of Cooperatively Rearranging Regions at the Glass Transition. *J. Non-Cryst. Solids* **1982**, *53 (3)*, 325-330. https://doi.org/10.1016/0022-3093(82)90089-8

[40] Saiter, A.; Delbreilh, L.; Couderc, H.; Arabeche, K.; Schönhals, A.; Saiter, J.-M. Temperature Dependence of the Characteristic Length Scale for Glassy Dynamics: Combination of Dielectric and Specific Heat Spectroscopy. *Phys. Rev. E* **2010**, *81 (4)*, 041805. https://doi.org/10.1103/PhysRevE.81.041805

[41] Codou, A.; Moncel, M.; Berkel, J. G. van; Guigo, N.; Sbirrazzuoli, N. Glass Transition Dynamics and Cooperativity Length of Poly(Ethylene 2,5-Furandicarboxylate) Compared to Poly(Ethylene Terephthalate). *Phys. Chem. Chem. Phys.* **2016**, *18 (25)*, 16647–16658. https://doi.org/10.1039/C6CP01227B

[42] Ginzburg, V.V. A simple mean-field model of glassy dynamics and glass transition. *Soft Matter* **2020**, *16*, 810. https://doi.org/10.1039/c9sm01575b

[43] Hempel, E.; Hempel, G.; Hensel, A.; Schick, C.; Donth, E. Characteristic Length of Dynamic Glass Transition near Tg for a Wide Assortment of Glass-Forming Substances. *J. Phys. Chem. B* **2000**, *104 (11)*, 2460-2466. https://doi.org/10.1021/jp991153f

[44] Schaumburg, G. Novocontrol Introduces High Quality Low Cost Interdigitated Comb Electrodes. *Dielectr. Newsl.* **2006**, *22*, 5-7.

[45] Havriliak, S.; Negami, S. A Complex Plane Analysis of α-Dispersions in Some Polymer Systems. *J. Polym. Sci. Part C Polym. Symp.* **1966**, *14 (1)*, 99-117. https://doi.org/10.1002/polc.5070140111

[46] Havriliak, S.; Negami, S. A Complex Plane Representation of Dielectric and Mechanical Relaxation Processes in Some Polymers. *Polymer* **1967**, *8*, 161-210. https://doi.org/10.1016/0032-3861(67)90021-3

[47] Alegría, A.; Goitiandia, L.; Tellería, I.; Colmenero, J. *α*-relaxation in the glass-transition range of amorphous polymers. 2. Influence of physical aging on the dielectric relaxation. *Macromolecules* **1997**, *30*, 3881-3887. https://doi.org/10.1021/ma961266m

[48] Alegría, A.; Goitiandia, L.; Colmenero, J. Interpretation of the TSDC fractional polarization experiments on the *α*-relaxation of polymers. *J. Polym. Sci. Part B: Polym. Phys.* **2000**, *38*, 2105-2133. https://doi.org/10.1002/1099-0488(20000815)38:16<2105::AID-POLB40>3.0.CO;2-7

[49] van Berkel, J.G.; Guigo, N.; Visser, H.A.; Sbirazzuoli, N. Chain Structure and Molecular Weight Dependent Mechanics of Poly(ethylene 2,5-furandicarboxylate) Compared to Poly(ethylene terephthalate). *Macromolecules* **2018**, *51 (21)*, 8539-8549. https://doi.org/10.1021/acs.macromol.8b01831

[50] Delpouve, N.; Saiter, A.; Dargent, E. Cooperativity Length Evolution during Crystallization of Poly(Lactic Acid). *Eur. Polym. J.* **2011**, *47 (12)*, 2414-2423. https://doi.org/10.1016/j.eurpolymj.2011.09.027

[51] Rijal, B.; Delbreilh, L.; Saiter, A. Dynamic Heterogeneity and Cooperative Length Scale at Dynamic Glass Transition in Glass Forming Liquids. *Macromolecules* **2015**, *48 (22)*, 8219-8231. https://doi.org/10.1021/acs.macromol.5b01152

[52] Raftopoulos, K.N.; Janowski, B.; Apekis, L.; Pielichowski, K.; Pissis, P. Molecular mobility and crystallinity in polytetramethylene ether glycol in the bulk and as soft component in polyurethanes. *Eur. Polym. J.* **2011**, *47 (11)*, 2120-2133. https://doi.org/10.1016/j.eurpolymj.2011.07.020

[53] Moura Ramos, J.J.; Diogo, H.P. Slow relaxations in semicrystalline poly(butylene succinate) below and above Tg. *Polym. Eng. Sci.* **2015**, *55 (8)*, 1873-1880.

https://doi.org/10.1002/pen.24027

[54] Capsal, J.F.; Dantras, E.; Dandurand, J.; Lacabanne, C. Dielectric relaxations and ferroelectric behaviour of even-odd polyamide PA 6,9. *Polymer* **2010**, *51 (20)*, 4606-4610. https://doi.org/10.1016/j.polymer.2010.07.040

[55] Sauer, B.B.; Avakian, P. Cooperative relaxations in amorphous polymers studied by thermally stimulated current depolarization. *Polymer* **1992**, *33 (24)*, 5128-5142. https://doi.org/10.1016/0032-3861(92)90793-V

[56] Capsal, J.F.; Dantras, E.; Lacabanne, C. Molecular mobility interpretation of the dielectric relaxor behavior in fluorinated copolymers and terpolymers. *J. Non-Cryst. Sol.* **2013**, *363*, 20-25. http://dx.doi.org/10.1016/j.jnoncrysol.2012.12.008

[57] Araujo, S.; Delpouve, N.; Dhotel, A.; Domeneke, S.; Guinault, A.; Delbreilh, L.; Dargent, E. Reducing the Gap between the Activation Energy Measured in the Liquid and the Glassy States by Adding a Plasticizer to Polylactide. *ACS Omega* **2018**, *3 (12)*, 17092-17099. https://doi.org/10.1021/acsomega.8b02474

[58] Soccio, M.; Martínez-Tong, D.E.; Alegría, A.; Munari, A.; Lotti, N. Molecular dynamics of fully biobased poly(butylene 2,5-furanoate) as revealed by broadband dielectric spectroscopy. *Polymer* **2017**, *128*, 24-30. https://doi.org/10.1016/j.polymer.2017.09.007

[59] Mackintosh, A.R.; Liggat, J.J. Dynamic Mechanical Analysis of Poly(Trimethylene Terephthalate): A Comparison with Poly(Ethylene Terephthalate) and Poly(Ethylene Naphthalate). *J. Appl. Polym. Sci.* **2004**, *92 (5)*, 2791-2796. https://doi.org/10.1002/app.20290

[60] Menegotto, J.; Demont, P.; Bernes, A.; Lacabanne, C. Combined dielectric spectroscopy and thermally stimulated currents studies of the secondary relaxation process in amorphous poly(ethylene terephthalate). *J. Polym. Sci. B: Polym. Phys.* **1999**, *37*, 3494-3503. https://doi.org/10.1002/(SICI)1099-0488(19991215)37:24<3494::AID-POLB10>3.0.CO;2-V

[61] Delbreilh, L.; Bernès, A.; Lacabanne, C. Secondary Retardation/Relaxation Processes in Bisphenol A Polycarbonate: Thermostimulated Creep and Dynamic Mechanical Analysis Combined Investigations. *Int. J. Polym. Anal. Charact.* **2005**, *10 (1-2)*, 41-56. https://doi.org/10.1080/10236660500345885

[62] Papamokos, G.; Dimitriadis, T.; Bikiaris, D.N.; Papageorgiou, G.Z.; Floudas, G. Chain Conformation, Molecular Dynamics, and Thermal Properties of Poly(n-methylene 2,5-furanoates) as a Function of Methylene Unit Sequence Length. *Macromolecules* **2019**, *52 (17)*, 6533-6546. https://doi.org/10.1021/acs.macromol.9b01320

[63] Genovese, L.; Soccio, M.; Lotti, N.; Munari, A.; Szymczyk, A.; Paszkiewicz, S.; Linares, A.; Nogales, A.; Ezquerra, T.A. Effect of chemical structure on the subglass relaxation

dynamics of biobased polyesters as revealed by dielectric spectroscopy: 2,5-furandicarboxylic acid vs. trans-1,4-cyclohexanedicarboxylic acid. *Phys. Chem. Chem. Phys.* **2018**, *20*, 15696-15706. https://doi.org/10.1039/C8CP01810C

[64] Nolasco, M.; Araujo, C.F.; Thiyagarajan, S.; Rudić, S.; Vaz, P.D.; Silvestre, A.J.D.; Ribeiro-Claro, P.J.A.; Sousa, A.F. Asymmetric Monomer, Amorphous Polymer? Structure-Property Relationships in 2,4-FDCA and 2,4-PEF, *Macromolecules* **2020**, *53*, 4, 1380-1387. https://doi.org/10.1021/acs.macromol.9b02449

[65] Starkweather, H. W.; Avakian, P.; Fontanella, J. J.; Wintersgill, M. C. Internal Motions in Polylactide and Related Polymers. *Macromolecules* **1993**, *26 (19)*, 5084-5087. https://doi.org/10.1021/ma00071a016

[66] Crétois, R.; Delbreilh, L.; Dargent, E.; Follain, N.; Lebrun, L.; Saiter, J. M. Dielectric Relaxations in Polyhydroxyalkanoates/Organoclay Nanocomposites. *Eur. Polym. J.* **2013**, *49 (11)*, 3434-3444. https://doi.org/10.1016/j.eurpolymj.2013.07.009

[67] Vogel, H. The law of the relation between the viscosity of liquids and the temperature. *Z. Phys.* **1921**, *22*, 645-646.

[68] Tammann, G.; Hesse, W. Die Abhängigkeit Der Viscosität von Der Temperatur Bie Unterkühlten Flüssigkeiten. *Z. Für Anorg. Allg. Chem.* **1926**, *156 (1)*, 245-257. https://doi.org/10.1002/zaac.19261560121

[69] Fulcher, G. S. Analysis of Recent Measurements of the Viscosity of Glasses. *J. Am. Ceram. Soc.* **1925**, *8 (6)*, 339-355. https://doi.org/10.1111/j.1151-2916.1925.tb16731.x

[70] Saiter, J. M.; Grenet, J.; Dargent, E.; Saiter, A.; Delbreilh, L. Glass Transition Temperature and Value of the Relaxation Time at Tg in Vitreous Polymers. *Macromol. Symp.* **2007**, *258 (1)*, 152-161. https://doi.org/10.1002/masy.200751217

[71] Leonardi, A.; Dantras, E.; Dandurand, J.; Lacabanne, C. Dielectric Relaxations in PEEK by Combined Dynamic Dielectric Spectroscopy and Thermally Stimulated Current. *J. Therm. Anal. Calorim.* **2013**, *111 (1)*, 807-814. https://doi.org/10.1007/s10973-012-2548-3

[72] Angell, C. A. Spectroscopy Simulation and Scattering, and the Medium Range Order Problem in Glass. *J. Non-Cryst. Solids* **1985**, *73 (1)*, 1-17. https://doi.org/10.1016/0022-3093(85)90334-5

[73] Schammé, B., Couvrat, N., Malpeli, P., Dudognon, E., Delbreilh, L., Dupray, V., Dargent, E., Coquerel, G. Transformation of an active pharmaceutical ingredient upon high-energy milling: a process-induced disorder in biclotymol. *Int. J. Pharm.* **2016**, *499*, 67-73. https://doi.org/10.1016/j.ijpharm.2015.12.032

[74] Schammé, B., Mignot, M., Couvrat, N., Tognetti, V., Joubert, L., Dupray, V., Delbreilh,

L., Dargent, E., Coquerel, G. Molecular Relaxations in Supercooled Liquid and Glassy States of Amorphous Quinidine: Dielectric Spectroscopy and Density Functional Theory Approaches. *J. Phys. Chem. B* **2016**, *120*, 7579-7592. https://doi.org/10.1021/acs.jpcb.6b04242

[75] Delbreilh, L.; Negahban, M.; Benzohra, M.; Lacabanne, C.; Saiter, J. M. Glass Transition Investigated by a Combined Protocol Using Thermostimulated Depolarization Currents and Differential Scanning Calorimetry. *J. Therm. Anal. Calorim.* **2009**, *96 (3)*, 865-871. https://doi.org/10.1007/s10973-009-0060-1

[76] Cowie, J.M.G.; Arrighi, V. Physical Aging of Polymer Blends. In: Utracki L., Wilkie C. (eds) *Polymer Blends Handbook*. Springer, Dordrecht, **2014**, pp. 1357-1394.

[77] Smith, G.D.; Bedrov, D. Relationship between the α- and β-relaxation processes in amorphous polymers: Insight from atomistic molecular dynamics simulations of 1,4-polybutadiene melts and blends. *J. Pol. Sci. Part B: Pol. Phys.* **2007**, *45 (6)*, 627-643. https://doi.org/10.1002/polb.21064

[78] Dargent, E.; Bureau, E.; Delbreilh, L.; Zumailan, A.; Saiter, J. M. Effect of Macromolecular Orientation on the Structural Relaxation Mechanisms of Poly(Ethylene Terephthalate). *Polymer* **2005**, *46 (9)*, 3090-3095. https://doi.org/10.1016/j.polymer.2005.01.096

[79] Couderc, H.; Delbreilh, L.; Saiter, A.; Grenet, J.; De Souza, N.; Saiter, J. M. Relaxation in Poly-(Ethylene Terephthalate Glycol)/Montmorillonite Nanocomposites Studied by Dielectric Methods. *J. Non-Cryst. Solids* **2007**, *353 (47)*, 4334-4338. https://doi.org/10.1016/j.jnoncrysol.2007.03.046

[80] Delbreilh, L.; Dargent, E.; Grenet, J.; Saiter, J.-M.; Bernès, A.; Lacabanne, C. Study of Poly(Bisphenol A Carbonate) Relaxation Kinetics at the Glass Transition Temperature. *Eur. Polym. J.* **2007**, *43 (1)*, 249-254. https://doi.org/10.1016/j.eurpolymj.2006.09.019

[81] Arnoult, M.; Dargent, E.; Mano, J. F. Mobile Amorphous Phase Fragility in Semi-Crystalline Polymers: Comparison of PET and PLLA. *Polymer* **2007**, *48 (4)*, 1012-1019. https://doi.org/10.1016/j.polymer.2006.12.053

[82] Puente, J. A. S.; Rijal, B.; Delbreilh, L.; Fatyeyeva, K.; Saiter, A.; Dargent, E. Segmental Mobility and Glass Transition of Poly(Ethylene-Vinyl Acetate) Copolymers: Is There a Continuum in the Dynamic Glass Transitions from PVAc to PE? *Polymer* **2015**, *76*, 213-219. https://doi.org/10.1016/j.polymer.2015.09.007

[83] Varol, N.; Monnier, X.; Delbreilh, L.; Saiter, A.; Fatyeyeva, K.; Dargent, E. Highlight of Primary and Secondary Relaxations in Amorphous Stereocomplex Polylactides. *Express*

Polym. Lett. **2020**, *14 (1)*, 48-62.

[84] Araujo, S.; Delpouve, N.; Domenek, S.; Guinault, A.; Golovchak, R.; Szatanik, R.; Ingram, A.; Fauchard, C.; Delbreilh, L.; Dargent, E. Cooperativity Scaling and Free Volume in Plasticized Polylactide. *Macromolecules* **2019**, *52 (16)*, 6107-6115. https://doi.org/10.1021/acs.macromol.9b00464

[85] Araujo, S.; Batteux, F.; Li, W.; Butterfield, L.; Delpouve, N.; Esposito, A.; Tan, L.; Saiter, J.M.; Negahban, M. A structural interpretation of the two components governing the kinetic fragility from the example of interpenetrated polymer networks. *J. Pol. Sci. Part B: Pol. Phys.* **2018**, *56 (20)*, 1393-1403. https://doi.org/10.1002/polb.24722

[86] Bouthegourd, E.; Esposito, A.; Lourdin, D.; Saiter, A.; Saiter, J. M. Size of the Cooperative Rearranging Regions vs. Fragility in Complex Glassy Systems: Influence of the Structure and the Molecular Interactions. *Phys. B Condens. Matter* **2013**, *425*, 83-89. https://doi.org/10.1016/j.physb.2013.05.029

[87] Esposito, A.; Delpouve, N.; Causin, V.; Dhotel,A.; Delbreilh, L.; Dargent, E. From a Three-Phase Model to a Continuous Description of Molecular Mobility in Semicrystalline Poly(hydroxybutyrate-co-hydroxyvalerate). *Macromolecules* **2016**, *49 (13)*, 4850-4861. https://doi.org/10.1021/acs.macromol.6b00384

[88] Floudas, G.; Fytas, G. Pressure-induced dynamic homogeneity in an athermal diblock copolymer melt. *J. Chem. Phys.* **1999**, *111*, 9129. https://doi.org/10.1063/1.479387

[89] Kremer, F.; Schönhals, A. (eds). *Broadband Dielectric Spectroscopy.* Springer-Verlag Berlin Heidelberg 2003. https://doi.org/10.1007/978-3-642-56120-7

[90] Xia, Y.; Cho, H.; R. S.H.; Bartl, M.H.; Sen, S. Coexistence of Structural and Dynamical Heterogeneity in Liquids Under Nanoconfinement. *Front. Phys.* **2020**, *8*, 130. https://doi.org/10.3389/fphy.2020.00130

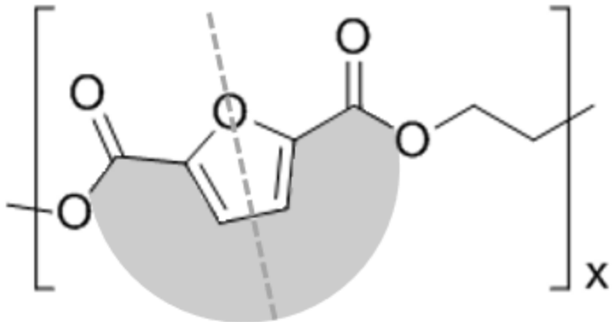

2,5-FDCA-based
HOMOPOLYMER

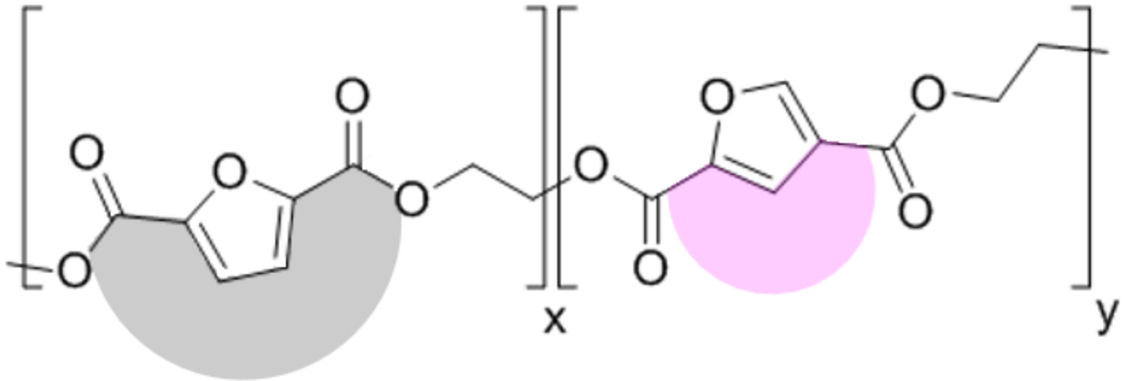

2,5-FDCA-based-*co*-2,4-FDCA-based
COPOLYMERS

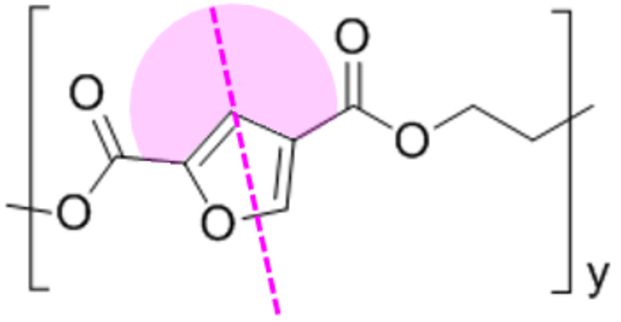

2,4-FDCA-based
HOMOPOLYMER